

Distributed dynamic event-based finite-time dissipative synchronization control for semi-Markov switched fuzzy cyber-physical systems against random packet losses

Xiru Wu(伍锡如), Yuchong Zhang(张煜翀), Tiantian Zhang(张烜烜), and Binlei Zhang(张斌磊)
Citation: Chin. Phys. B, 2023, 32 (**10**): 100506. DOI: 10.1088/1674-1056/acb91b
Journal homepage: http://cpb.iphy.ac.cn; http://iopscience.iop.org/cpb

What follows is a list of articles you may be interested in

Turing/Turing-like patterns: Products of random aggregation of spatial components

Jian Gao(高见), Xin Wang(王欣), Xinshuang Liu(刘心爽), and Chuansheng Shen(申传胜)
Chin. Phys. B, 2023, 32 (**7**): 070503. DOI: 10.1088/1674-1056/acc0f9

Synchronization-desynchronization transitions in networks of circle maps with sinusoidal coupling

Yun Zhai(翟云), Jinghua Xiao(肖井华), and Zhigang Zheng(郑志刚)
Chin. Phys. B, 2023, 32 (**6**): 060505. DOI: 10.1088/1674-1056/acc062

Finite-time synchronization of uncertain fractional-order multi-weighted complex networks with external disturbances via adaptive quantized control

Hongwei Zhang(张红伟), Ran Cheng(程然), and Dawei Ding(丁大为)
Chin. Phys. B, 2022, 31 (**10**): 100504. DOI: 10.1088/1674-1056/ac686b

Dynamic modeling and aperiodically intermittent strategy for adaptive finite-time synchronization control of the multi-weighted complex transportation networks with multiple delays

Ning Li(李宁), Haiyi Sun(孙海义), Xin Jing(靖新), and Zhongtang Chen(陈仲堂)
Chin. Phys. B, 2021, 30 (**9**): 090507. DOI: 10.1088/1674-1056/abea92

Finite-time sliding mode synchronization of chaotic systems

Ni Jun-Kang (倪骏康), Liu Chong-Xin (刘崇新), Liu Kai (刘凯), Liu Ling (刘凌)
Chin. Phys. B, 2014, 23 (**10**): 100504. DOI: 10.1088/1674-1056/23/10/100504

Distributed dynamic event-based finite-time dissipative synchronization control for semi-Markov switched fuzzy cyber-physical systems against random packet losses

Xiru Wu(伍锡如), Yuchong Zhang(张煜翀)†, Tiantian Zhang(张畑畑), and Binlei Zhang(张斌磊)

School of Electronic Engineering and Automation, Guilin University of Electronic Technology, Guilin 541004, *China*

(Received 25 October 2022; revised manuscript received 22 January 2023; accepted manuscript online 6 February 2023)

This paper is concerned with the finite-time dissipative synchronization control problem of semi-Markov switched cyber-physical systems in the presence of packet losses, which is constructed by the Takagi–Sugeno fuzzy model. To save the network communication burden, a distributed dynamic event-triggered mechanism is developed to restrain the information update. Besides, random packet dropouts following the Bernoulli distribution are assumed to occur in sensor to controller channels, where the triggered control input is analyzed via an equivalent method containing a new stochastic variable. By establishing the mode-dependent Lyapunov–Krasovskii functional with augmented terms, the finite-time boundness of the error system limited to strict dissipativity is studied. As a result of the help of an extended reciprocally convex matrix inequality technique, less conservative criteria in terms of linear matrix inequalities are deduced to calculate the desired control gains. Finally, two examples in regard to practical systems are provided to display the effectiveness of the proposed theory.

Keywords: cyber-physical systems, finite-time synchronization, distributed dynamic event-triggered mechanism, random packet losses

PACS: 05.45.Xt, 07.05.Mh, 07.05.Dz, 05.45.–a **DOI:** 10.1088/1674-1056/acb91b

1. Introduction

Cyber-physical systems (CPSs), as the complex systems integrating computation, networks communication and control,[1,2] have been investigated intensively due to their frequent applications in network coordination and physical resources, such as network power schedules, multi-agent control and remote estimation.[3–5] It is worth noting that reliability has become the increasingly critical network-induced issue in the control of real CPSs. In Refs. [6,7], the sliding mode control approach was deployed for CPSs with malicious attacks to guarantee security and reliability. In particular, bandwidth limitation is becoming a serious problem due to the physical properties of network interaction, which generates inevitable information packet losses. Nevertheless, current research rarely refers to the effect of random packet losses in CPSs, aside from the interconnected multi-systems with complex structure.

The Takagi–Sugeno (T-S) fuzzy model has been used to handle complex nonlinear systems due to its remarkable competence in accurate approximation.[8–10] Reference [11] built the model of partially coupled complex networks via a collection of IF-THEN rules and fuzzy membership functions. To solve the immeasurable state problem, Ref. [12] also developed an adaptive fuzzy observer using IF-THEN fuzzy rules. The T-S fuzzy model was applied in the resilient controller design of CPSs to deal with input saturation and cyberattack in Ref. [13]. In reality, abrupt changes in system structure may lead to unexpected mode variation and system instability, such that Markov switched parameters are introduced to organize the T-S fuzzy system model.[14,15] In Ref. [14], a finite-time asynchronous state estimation scheme was raised for Markov jump T-S fuzzy systems. As reported in Ref. [16], the transition probability matrix is considered to be time-varying because the sojourn time obeys arbitrary probability distributions. In view of this, semi-Markov switched T-S fuzzy systems have more relaxed constraint compared with conventional ones.[17,18] For instance, in Ref. [17], Zhang *et al.* concerned the stabilization issue of uncertain T-S fuzzy systems under a semi-Markov chain. Therefore, it is meaningful to further explore the effective control theory in T-S fuzzy CPSs (TSFCPSs) subject to semi-Markov switched modes.

In the study of system stability control, most of the existing results focused on Lyapunov stability within an infinite time interval, but some realistic scenes require finite-time control performance. The authors in Ref. [19] applied a power integrator technique combined with a backstepping method to achieve finite-time stability control. Such a theory has been imported to finite-time synchronization (FTS) and, simultaneously, it should also be emphasized that consideration of system properties in the achievement of FTS is necessary.[20,21] As the description of the immanent relationship between storage functions and supply rates, dissipativity performance can reflect the internal stability and has been regarded as a more powerful tool in system control than passivity

†Corresponding author. E-mail: yczhang_1128@163.com

© 2023 Chinese Physical Society and IOP Publishing Ltd

and $H\infty$ theory.[22] With regard to a class of Markovian jump inertial neural networks, Song *et al.* derived the less conservative criterion of FTS with a dissipative index in Ref. [23]. As reported in Ref. [24], the global dissipativity based on the Filippov solution was developed to ensure the FTS of memristor-based neural networks. However, the dissipative problem of FTS control for TSFCPSs has not attracted adequate attention.

To cope with the limited communication resources, an event-triggered mechanism (ETM) was proposed to reduce frequent data transmission and overmuch consumption.[25–28] By this means, the updated data of the control input are released only when a prespecified trigger condition is satisfied. In Ref. [29], based on adaptive ETM, the authors proposed a quantized method for the distributed estimation of semi-Markov switched sensor networks. With the event-based control technique, the stability problem of linear systems suffering packet losses was solved in Ref. [30]. In recent literature, a class of dynamic ETM was designed by setting an internal iterative variable in the triggering condition, which possesses lower triggering frequency than conventional ETM.[31–33] As shown in Ref. [33], the authors proposed a $H\infty$ filtering strategy for a T-S fuzzy system based on dynamic ETM, which contributed to reduction of the consumption. Although the dynamic ETM has shown superiority, some redundant data will be transmitted if subsystems share a unified triggering condition, which promotes the motivation for extending related studies under the distributed framework.[34–36] Besides, the process of packet dropout is depicted by a stochastic sequence following the continuous Bernoulli distribution in previous studies like Refs. [37–39], but this method is unsuitable for a non-uniform sampling situation where triggering instants fail to be transmitted. Therefore, there is the need to establish a realistic framework to analyze a distributed dynamic ETM (DDETM) influenced by random packet losses in semi-Markov switched TSFCPSs.

According to the aforementioned analysis, this paper aims to investigate the strictly dissipative FTS issue of semi-Markov switched TSFCPSs with packet dropouts under a distributed dynamic event-based pinning control scheme. The main contributions are summarized as follows:

1) To investigate the finite-time synchronization strategy within the framework of CPSs with interconnected multi-systems, a T-S fuzzy model-based distributed control construction is developed. In contrast to the network models in Refs. [21,42], the presented system considers parameters subject to a semi-Markov chain and a communication process restrained by packet loss simultaneously.

2) The pinning strategy and DDETM are jointly proposed to improve the transmission schedule of desired controller signals. Unlike the approaches in Refs. [25–27], a dynamic variable related to synchronization errors is introduced to design the triggering condition, which results in a lower information update frequency. Additionally, aiming to handle the stochastic data loss sequence that does not satisfy Bernoulli distribution, an equivalent prediction model distinguished from Refs. [37–39] is provided to transform the triggering instant.

3) Based on augmented terms with respect to delays, a mode-dependent Lyapunov–Krasovskii functional (LKF) is constructed to guarantee the FTS accompanied by the desired dissipative performance. Compared with the sum-term estimation methods in Refs. [11,27,31,43], an extended reciprocally convex matrix inequality (ERCMI) is combined with a delay-product-type double sum term to derive a tighter result with less conservatism.

The rest of this paper is arranged as follows: Section 2 describes the preliminaries and builds the problem model. In Section 3, synchronization and dissipativity analysis of closed-loop TSFCPSs proceed via strict mathematical derivations. Section 4 provides two examples to verify the theoretical results. Section 5 gives the conclusions.

Notations Throughout the paper, $\mathbb{R}^n$ and $\mathbb{R}^{n\times m}$ represent the n-dimensional Euclidean space and the set of all $n\times m$ dimensional real matrices; $\mathbb{Z}^+$ denotes the set of all positive integers; $l_2[0,\infty)$ means the space of square-summable infinite vector functions over $[0,\infty)$; $\mathrm{vec}_n\{\cdot\}$ is the symbol of the column vector, including n blocks; $\mathrm{diag}\{\cdot\}$ means a block-diagonal matrix; $\otimes$ refers to the Kronecker product; $c_{\max}(R)$ $(c_{\min}(R))$ represents the maximum eigenvalue (minimum eigenvalue) of the matrix R; $\Pr\{\cdot\}$ and $\mathcal{E}\{\cdot\}$ represent the probability of event occurrence and mathematical expectation, respectively; $\mathrm{Sym}\{P\}=P^{\mathrm{T}}+P$; and $*$ denotes the symmetric term of a symmetric matrix. In addition, the matrix $Q>0$ $(Q<0)$ means Q is a positive-definite matrix (negative-definite matrix).

2. Problem formulation and preliminaries

Consider a class of semi-Markovian switched discrete-time complex networks with N coupled nodes as the CPSs, which can be described by the following T-S fuzzy rules:

Plant rule m: If $\kappa_1(k)$ is $\mathcal{G}_1^m$, $\kappa_2(k)$ is $\mathcal{G}_2^m$, …, and $\kappa_p(k)$ is $\mathcal{G}_p^m$, then

$$\begin{cases} x_i(k+1) = A_m^{\lambda(k)}x_i(k) + B_m^{\lambda(k)}f(x_i(k)) \\ \qquad\qquad + D_m^{\lambda(k)}h(x_i(k-\sigma(k))) \\ \qquad\qquad + \sum\limits_{j=1}^{N} g_{ij}^{\lambda(k)}Lx_i(k) + R_m^{\lambda(k)}u_i(k) \\ \qquad\qquad + O_m^{\lambda(k)}\omega_i(k) + J^{\lambda(k)}, \\ y_i(k) = C_m^{\lambda(k)}x_i(k) + E_m^{\lambda(k)}\omega(k), \\ x_i(s) = \nu_i(s),\ s\in\{-\bar{\sigma},-\bar{\sigma}+1,\ldots,0\}, \end{cases} \tag{1}$$

where $\kappa(k)=\{\kappa_1(k),\kappa_2(k),\ldots,\kappa_p(k)\}$ denotes the premise

variables, $\mathcal{G}_1^m$, $\mathcal{G}_2^m$, …, $\mathcal{G}_p^m$ are the fuzzy sets described by membership variables with $m = 1,2,\ldots,r$ and r is the number of fuzzy rules. Here, $x_i(k) \in \mathbb{R}^n$, $y_i(k) \in \mathbb{R}^y$, $u_i(k) \in \mathbb{R}^n$ are the state vector, controlled output vector and controller signal of the ith node, respectively; $\sigma(k)$ represents the time-varying delays appearing in dynamic behavior; $\omega_i(k) \in \mathbb{R}^{n\omega}$ is the disturbance input vector; and $J^{\lambda(k)} \in \mathbb{R}^n$ is the external input vector. Meanwhile, $f(x_i(k)) = \mathrm{vec}_n\{f_i(x_i(k))\}$ and $h(x_i(k-\sigma(k))) = \mathrm{vec}_n\{h_i(x_i(k-\sigma(k)))\}$ are the non-delayed and delayed node activation functions. Here, $\nu_i(s)$ is the initial condition of presented CPSs, L stands for the inner coupled parameter matrix and $G^{\lambda(k)} = (g_{ij}^{\lambda(k)})_{N\times N} \in \mathbb{R}^{N\times N}$ is the outer coupling matrix of the network structure, where $g_{ij}^{\lambda(k)} \geq 0, i \neq j$ and $\sum_{j=1}^N g_{ij}^{\lambda(k)} = 0$. Meanwhile, $A_m^{\lambda(k)}$, $B_m^{\lambda(k)}$, $C_m^{\lambda(k)}$, $D_m^{\lambda(k)}$, $E_m^{\lambda(k)}$, $R_m^{\lambda(k)}$ and $O_m^{\lambda(k)}$ are weight matrices with appropriate dimensions, which follows the semi-Markov process $\{\lambda(k), k \geq 0\}$ within a finite set $\mathcal{V} = \{1,2,\ldots,v\}$.

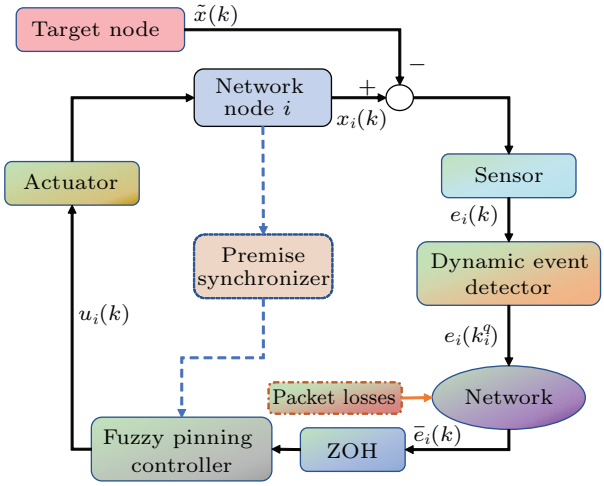


Fig. 1. A block diagram of the control procedure in node i.

Some essential conditions are highlighted as follows:

(A_1) For the time-varying delay $\sigma(k)$, there are several constants $\bar{\sigma}$, $\underline{\sigma}$, τ and $\bar{\tau}$ satisfying $0 \leq \underline{\sigma} \leq \sigma(k) \leq \bar{\sigma}$ and $\underline{\tau} \leq \tau(k) \leq \bar{\tau}$, where $\tau(k)$ is defined as $\sigma(k+1) - \sigma(k)$. For simplification, set $\Delta_\sigma = \bar{\sigma} - \underline{\sigma}$, $\sigma = \sigma(k)$ and $\tau = \tau(k)$.

(A_2) The nonlinear node activation functions $f_i(\cdot)$ and $h_i(\cdot)$ are restrained by the following global Lipschitz condition for $\forall a_1, a_2, b_1, b_2 \in \mathbb{R}$ with $a_1 \neq a_2$, $b_1 \neq b_2$:

$$\alpha_l^- \leq \frac{f_l(a_1) - f_l(a_2)}{a_1 - a_2} \leq \alpha_l^+, \quad \beta_l^- \leq \frac{h_l(b_1) - h_l(b_2)}{b_1 - b_2} \leq \beta_l^+,$$

where α_l^-, α_l^+, β_l^- and β_l^+ are stated constant scalars.

(A_3) The discrete semi-Markov chain $\{\lambda(k), k \geq 0\}$ is right-continuous and the mode switching complies with the transition probability $\Pr\{\lambda(k+1) = s | \lambda(k) = t\} = \psi_{st}(k)$, where $\psi_{st}(k) \in [0,1]$, $\forall s,t \in \mathcal{V}$, is regulated by the properties $\sum_{s=1}^v \psi_{st}(k) = 1$, $\psi_{st}^- \leq \psi_{st}(k) \leq \psi_{st}^+$.

As $\psi_{st}(k)$ is time-varying with incomplete measuring information, it can be expressed by the following new form:

$$\psi_{st}(k) = \sum_\ell^{\mathcal{L}} \mu_\ell \psi_{st}^\ell, \quad \sum_\ell^{\mathcal{L}} \mu_\ell = 1$$

for $\mu_\ell \geq 0$. Based on Refs. [16,18,22], ψ_{st}^ℓ is limited by the following boundary conditions:

$$\psi_{st}^\ell = \begin{cases} \psi_{st}^- + (\ell-1)\dfrac{\psi_{st}^+ - \psi_{st}^-}{\mathcal{L}-1}, & s \neq t, \\ \psi_{st}^+ + (\ell-1)\dfrac{\psi_{st}^+ - \psi_{st}^-}{\mathcal{L}-1}, & s = t. \end{cases} \tag{2}$$

Via the weighted average fuzzy blending method, the global TSFCPSs model with respect to subsystem (1) is described as

$$\begin{cases} x_i(k+1) = \sum_{m=1}^r \Im_m \big[A_m^{\lambda(k)} x_i(k) + B_m^{\lambda(k)} f(x_i(k)) \\ \qquad + D_m^{\lambda(k)} h(x_i(k-\sigma))) \\ \qquad + \sum_{j=1}^N g_{ij}^{\lambda(k)} L x_i(k) + R_m^{\lambda(k)} u_i(k) \\ \qquad + O_m^{\lambda(k)} \omega_i(k) + J^{\lambda(k)}\big], \\ y_i(k) = \sum_{m=1}^r \Im_m \big[C_m^{\lambda(k)} x_i(k) + E_m^{\lambda(k)} \omega(k)\big], \end{cases} \tag{3}$$

where $\Im_m$ represents the simplification of the normalized membership function $\Im_m(\kappa(k))$ satisfying

$$\Im_m(\kappa(k)) = \frac{\prod_h^p \mathcal{F}_m^h(\kappa_h(k))}{\sum_j^r \prod_j^p \mathcal{F}_j^h(\kappa_h(k))},$$

in which $\mathcal{F}_m^h(\kappa_h(k))$ is the membership degree of $\kappa_h(k)$ in $\mathcal{F}_m^h$. From the definition of fuzzy sets, $\prod_h^p \mathcal{F}_m^h(\kappa_h(k)) > 0$, such that $\Im_m(\kappa(k)) \in (0,1)$ and $\sum_{m=1}^r \Im_m(\kappa(k)) = 1$.

The model of the target node in TSFCPSs is given as

$$\begin{cases} \tilde{x}(k+1) = \sum_{m=1}^r \Im_m \big[A_m^{\lambda(k)} \tilde{x}(k) + B_m^{\lambda(k)} f(\tilde{x}(k)) \\ \qquad + D_m^{\lambda(k)} h(\tilde{x}(k-\sigma)) + J^{\lambda(k)}\big], \\ \tilde{y}(k) = \sum_{m=1}^r \Im_m C_m^{\lambda(k)} \tilde{x}(k), \end{cases} \tag{4}$$

where $\tilde{x}(k) \in \mathbb{R}^n$, $\tilde{y}(k) \in \mathbb{R}^y$ are vectors on behalf of the target state and corresponding control output, respectively. The initial state of $\tilde{x}(k)$ is set as $\tilde{\nu}(s)$ for $s \in \{-\bar{\sigma}, -\bar{\sigma}+1, \ldots, 0\}$.

We define $e_i(k) = x_i(k) - \tilde{x}(k)$ and $e_{yi} = y_i(k) - \tilde{y}(k)$, such that we obtain the synchronization error system of TSFCPSs

as below:

$$\begin{cases} e_i(k+1) = \sum\limits_{m=1}^{r} \Im_m \big[A_m^{\lambda(k)} e_i(k) + B_m^{\lambda(k)} \tilde{f}(e_i(k)) \\ \qquad + D_m^{\lambda(k)} \tilde{h}(e_i(k-\sigma)) \\ \qquad + \sum\limits_{j=1}^{N} g_{ij}^{\lambda(k)} L e_i(k) + R_m^{\lambda(k)} u_i(k) \\ \qquad + O_m^{\lambda(k)} \omega_i(k)\big], \\ e_{yi}(k) = \sum\limits_{m=1}^{r} \Im_m \left[C_m^{\lambda(k)} e_i(k) + E_m^{\lambda(k)} \omega_i(k)\right], \end{cases} \tag{5}$$

where $\tilde{f}(e_i(k)) = f(x_i(k)) - f(\tilde{x}(k))$, $\tilde{h}(e_i(k-\sigma)) = h(x_i(k-\sigma)) - h(\tilde{x}(k-\sigma))$. The block diagram of controlled node i is plotted in Fig. 1.

To compensate the lost data caused by packet losses, the estimated error is introduced to the controller design. Combined with the parallel distribution control (PDC) technology, the fuzzy pinning controller can be given by the following rules:

Controller rule v: If $\kappa_1(k)$ is $\mathcal{G}_1^v$, $\kappa_2(k)$ is $\mathcal{G}_1^v$, ..., and $\kappa_p(k)$ is $\mathcal{G}_p^v$, then

$$u_i(k) = -\varphi_i K_{i,v}^{\lambda(k)} \bar{e}_i(k), \tag{6}$$

where $\bar{e}_i(k)$ is the estimated control input and $K_{i,v}^{\lambda_k}$ is the ith control gain matrix under the fuzzy rule v. Besides, φ_i is the pinning parameter, where $\varphi_i = 1$ means the ith node is controlled, otherwise $\varphi_i = 0$.

The distributed event generator function $Q(\cdot,\cdot)$ is regulated as follows:

$$Q(e_i(k), \delta_i) = \varepsilon_i^{\mathrm{T}}(k)\varepsilon_i(k) - \delta_i e_i^{\mathrm{T}}(k) e_i(k), \tag{7}$$

where $\varepsilon_i(k) = e_i(k) - e_i(k_i^q)$ and δ_i is a settled positive scalar. Therein, k_i^q denotes the qth triggered instant of the ith node and k_i^{q+1} is the next triggered instant with $k_i^0 = 0$, $k_i^q < k_i^{q+1}$. The update instants of the controller are decided iteratively by the following event-triggered constraint:

$$\begin{aligned} k_i^{q+1} &= \inf\left\{ k \in \mathbb{Z}^+ \,\middle|\, k > k_i^q,\ Q(e_i(k), \delta_i) - \frac{\Gamma_i(k)}{\hat{\rho}_i} \geq 0 \right\}, \\ & k_i^0 = 0. \end{aligned} \tag{8}$$

Here, $\hat{\rho}_i$ is a given positive parameter, and $\Gamma_i(k)$ represents the ith internal dynamic variable, which is described as

$$\Gamma_i(k+1) = \eta_i \Gamma_i(k) + \delta_i e_i^{\mathrm{T}}(k) e_i(k) - \varepsilon_i^{\mathrm{T}}(k)\varepsilon_i(k) \tag{9}$$

with $\Gamma_i(0) = \Gamma_i^0 \geq 0$ and the given constant $\eta_i \in (0,1)$.

Remark 1 Compared with the traditional ETMs, shown in Refs. [25–27], restricted by a static-coefficient-related triggering threshold, the adopted DDETM is established under a time-varying constraint condition, where the dynamic variable $\Gamma_i(k)$ is influenced by the real-time system errors $e_i(k)$ and $\varepsilon_i(k)$. It is obvious from Eq. (8) that the triggering mechanism will reduce to the static ETM in Ref. [27] if parameter $\hat{\rho}_i$ goes to infinity. Therefore, the DDETM can flexibly regulate the distributed controller performance by changing parameters δ_i and $\hat{\rho}_i$. It easily observes that the value of δ_i increases together with the decrease of the triggering rate, while the triggering rate increases with the growth of $\hat{\rho}_i$.

Since the controller signal will be updated when the triggering condition (8) is satisfied, the packet loss only occurs on triggering instants. Therefore, during the triggering interval $[k_i^q, k_i^{q+1})$, there are two issues for the prediction of control input $\bar{e}_i(k)$:

1) If $k = k_i^q$, $\bar{e}_i(k_i^q) = \rho_i(k_i^q) e_i(k_i^q) + (1 - \rho_i(k_i^q))\bar{e}_i(k_i^q - 1)$.

2) If $k \in (k_i^q, k_i^{q+1})$, $\bar{e}_i(k) = \bar{e}_i(k-1) = \bar{e}_i(k_i^q)$,

where $\bar{e}_i(-1)$ is the initial condition with a value of zero in this paper, the stochastic variable $\rho_i(k_i^q)$ taking values of 1 or 0 is independent and follows the Bernoulli process with $\Pr\{\rho_i(k_i^q) = 1\} = \tilde{\rho}$ and $\Pr\{\rho_i(k_i^q) = 0\} = 1 - \tilde{\rho}$ for $\tilde{\rho} \in [0,1]$. By considering these two cases, the ith control input is defined as

$$\bar{e}_i(k) = \rho_i(k_i^q) e_i(k_i^q) + (1 - \rho_i(k_i^q))\bar{e}_i(k-1), \tag{10}$$

where $k \in [k_i^q, k_i^{q+1})$. In addition, the updated input signal cannot be transmitted to the controller before the next triggered instant, such that the value of $\rho_i(k_i^q)$ remains constant within $[k_i^q, k_i^{q+1})$. We define a new stochastic variable $\chi(k)$ and the predicted control input is described as follows for $\forall k \in [k_i^q, k_i^{q+1})$:

$$\bar{e}_i(k) = \chi_i(k)(e_i(k) - \varepsilon_i(k)) + (1 - \chi_i(k))\bar{e}_i(k-1), \tag{11}$$

where $\{\chi_i(k)\}_{k\in\mathbb{Z}^+} = \{\chi_i(0), \chi_i(1), \ldots, \chi_i(t), \ldots\}$ with $\chi_i(t) = \rho_i(k_i^q)$ for $t \in [q+1+l(q), q+1+l(q)+l_i^{i+1}]$ and $l(q) = l_0^1 + l_1^2 + \cdots + l_{i-1}^i$. It should be stressed that $\Pr\{\chi_i(k) = 1\} = \Pr\{\rho_i(k_i^q) = 1\} = \tilde{\rho}_i$ and $\Pr\{\chi_i(k) = 0\} = \Pr\{\rho_i(k_i^q) = 0\} = 1 - \tilde{\rho}_i$. Thus, the control signal affected by dropped information is rewritten as

$$\begin{aligned} u_i(k) \ = \ & -\sum_{v=1}^{r} \Im_v \varphi_i \big\{ K_{i,v}^{\lambda(k)} \chi_i(k)(e_i(k) - \varepsilon_i(k)) \\ & + K_{i,v}^{\lambda(k)} (1 - \chi_i(k)) \bar{e}_i(k-1) \big\}. \end{aligned} \tag{12}$$

The controller dynamics can be obtained by computing $e_i(k)$ in the interval of $[k_i^q, k_i^{q+1})$ for the availability of $e_i(k_i^q)$. Therefore, controller (12) can share the same premise variables $\kappa_i(k)$ with system (1).

Remark 2 Combined with the packet dropout behavior, the controller limited by the event-triggered condition will receive a relatively less feasible data packet from the sensor. It is worth noting that triggering instants are non-uniform sequences, such that the continuous Bernoulli distribution model in Refs. [8,29,38] cannot be directly employed to describe the event-based controller. By constructing a new sequence

$\{\chi(k)\}_{k\in\mathbb{Z}^+}$ in regard to variable $k\in[k_i^q,k_i^{q+1})$, the circumstance of triggered data transmission will be captured adequately.

Remark 3 In view of the concept of the ETM, premise variables of the system usually differ from those in the controller due to various time scales of $e_i(k)$ and $e_i(k_i^q)$. Thus, some of the literature, like Ref. [25], chose different premise variables, which may lead to needless complexity. Notice that $e_i(k)$ depends on $e_i(k_i^q)$ for $k\in[k_i^q,k_i^{q+1})$, and this paper deploys a premise synchronizer for controller (12) to set its premise variables approximate to the system's.

Substituting Eq. (11) into Eq. (5), and letting $e(k)=\mathrm{col}_N\{e_i^{\mathrm{T}}(k)\}$, $F(e(k))=\mathrm{col}_N\{\tilde{f}_i(e_i(k))\}$, $H(e(k-\sigma))=\mathrm{col}_N\{\tilde{h}_i^{\mathrm{T}}(e_i(k-\sigma))\}$, $\omega(k)=\mathrm{col}_N\{\omega_i^{\mathrm{T}}(k)\}$, $\Sigma(k)=\mathrm{diag}_N\{\tilde{\chi}_i(k)\}$, $\tilde{\chi}_i(k)=I_n\cdot\tilde{\rho}_i$, $\mathcal{K}_v^{\lambda(k)}=\mathrm{diag}_N\{\varphi_i K_{i,v}^{\lambda(k)}\}$, the simplified closed-loop system is presented as follows:

$$\begin{cases} e(k+1)=\sum\limits_{m=1}^{r}\sum\limits_{v=1}^{r}\Im_m\Im_v\big[(\boldsymbol{A}_m^{\lambda(k)}-\boldsymbol{R}_m^{\lambda(k)}\mathcal{K}_v^{\lambda(k)}\Sigma(k)\\ \qquad +G^{\lambda(k)}\otimes L)e(k)+\boldsymbol{B}_m^{\lambda(k)}F(e(k))\\ \qquad +\boldsymbol{D}_m^{\lambda(k)}H(e(k-\sigma))+\boldsymbol{O}_m^{\lambda(k)}\omega(k)\\ \qquad +\boldsymbol{R}_m^{\lambda(k)}\mathcal{K}_v^{\lambda(k)}\Sigma(k)\varepsilon(k)\\ \qquad -\boldsymbol{R}_m^{\lambda(k)}\mathcal{K}_v^{\lambda(k)}(I-\Sigma(k))\bar{e}(k-1)\big],\\ e_y(k)=\sum\limits_{m=1}^{r}\Im_m\big[\boldsymbol{C}_m^{\lambda(k)}e(k)+\boldsymbol{E}_m^{\lambda(k)}\omega(k)\big], \end{cases} \tag{13}$$

where some Kronecker products are set as $\boldsymbol{A}_m^{\lambda(k)}=I_N\otimes A_m^{\lambda(k)}$, $\boldsymbol{B}_m^{\lambda(k)}=I_N\otimes B_m^{\lambda(k)}$, $\boldsymbol{D}_m^{\lambda(k)}=I_N\otimes D_m^{\lambda(k)}$, $\boldsymbol{O}_m^{\lambda(k)}=I_N\otimes O_m^{\lambda(k)}$, $\boldsymbol{R}_m^{\lambda(k)}=I_N\otimes R_m^{\lambda(k)}$, $\boldsymbol{C}_m^{\lambda(k)}=I_N\otimes C_m^{\lambda(k)}$ and $\boldsymbol{E}_m^{\lambda(k)}=I_N\otimes E_m^{\lambda(k)}$.

Figure 2 demonstrates the operation framework of the closed-loop system, where the DDETM is proposed to manage the signal transmission. Moreover, a compensation mechanism is employed in the control input to guarantee the reliability.

Before conducting further analysis, some essential definitions, assumptions and lemmas are listed.

Definition 1[20] There is a matrix $\mathcal{Q}$, a given constant $\tilde{\omega}$ and two positive scalars ε_1, ε_2 with $\varepsilon_1<\varepsilon_2$. The error system (13) is said to be mean-square finite-time bounded with respect to $(\varepsilon_1,\varepsilon_2,\mathcal{X},\mathcal{T},\tilde{\omega})$ if the following condition is insured for $\forall k\in\{1,2,\ldots,\mathcal{T}\}$:

$$\begin{cases} \sup\limits_{\iota=\{-\bar{\sigma},-\bar{\sigma}+1,\ldots,0\}}\mathcal{E}\{e^{\mathrm{T}}(\iota)\mathcal{X}e(\iota)\}\le\varepsilon_1\\ \sum\limits_{k=0}^{\mathcal{T}}\omega^{\mathrm{T}}(k)\omega(k)\le\tilde{\omega} \end{cases}\Rightarrow\mathcal{E}\{e^{\mathrm{T}}(k)\mathcal{X}e(k)\}\le\varepsilon_2. \tag{14}$$

Definition 2[22] Given a fixed scalar $\gamma>0$, the real matrices $\Upsilon_1=\Upsilon_1^{\mathrm{T}}\le 0$, Υ_2 and $\Upsilon_3=\Upsilon_3^{\mathrm{T}}$, system (1) with disturbance $\omega(k)\in l_2[0,\infty)$ can achieve the strictly $(\Upsilon_1,\Upsilon_2,\Upsilon_3)$–$\gamma$–dissipative FTS with respect to $(\epsilon_1,\epsilon_2,\mathcal{X},\mathcal{T},\tilde{\omega},\gamma)$ if error system (13) satisfies the condition of Definition 1 and the following inequation for all $\mathcal{T}\ge 0$:

$$\sum_{k=0}^{\mathcal{T}}\mathcal{E}\{\mathcal{J}(e_y(k),\omega(k))\}\ge\gamma\sum_{k=0}^{\mathcal{T}}\omega^{\mathrm{T}}(k)\omega(k), \tag{15}$$

where the energy supply rate $\mathcal{J}(e_y(k),\omega(k))$ is denoted as

$$\begin{aligned}&\mathcal{J}(e_y(k),\omega(k))\\ &=e_y^{\mathrm{T}}(k)\Upsilon_1 e_y(k)+2e_y^{\mathrm{T}}(k)\Upsilon_2\omega(k)+\omega^{\mathrm{T}}(k)\Upsilon_3\omega(k).\end{aligned}$$

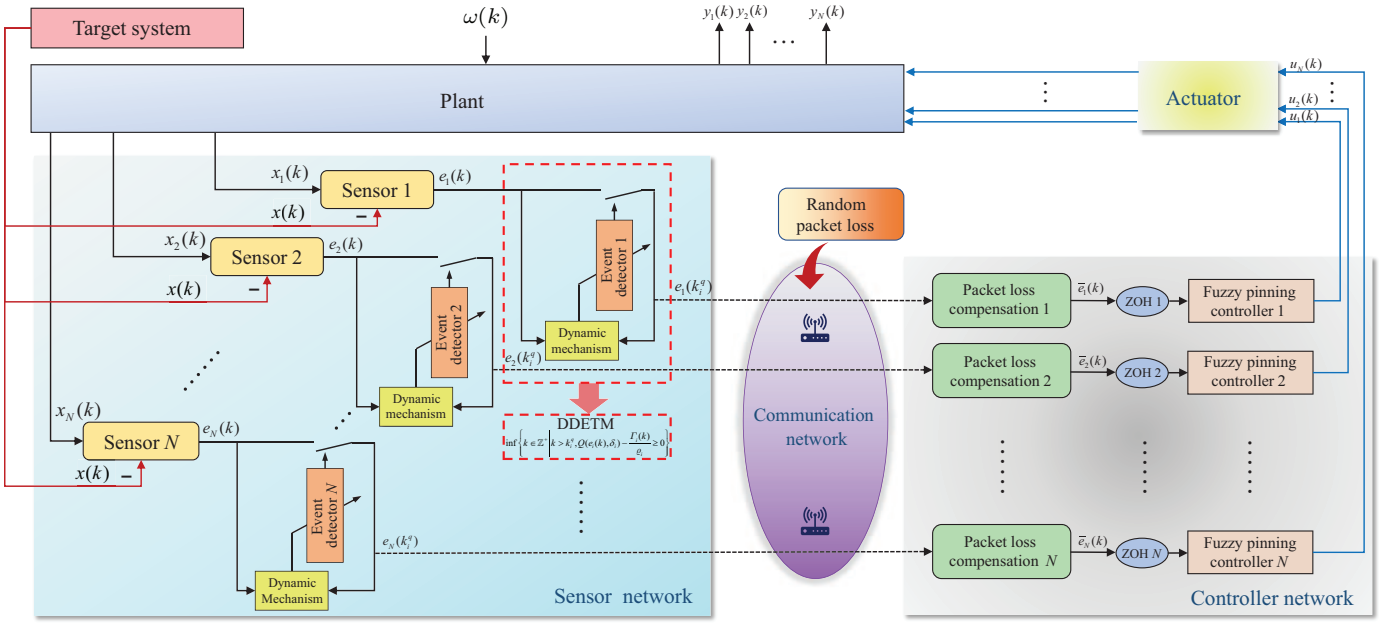


Fig. 2. The framework of detailed signal transmission in the whole closed-loop CPSs.

Assumption 1 The initial value of the error system should conform to the following condition:

$$\mathcal{E}\left\{\psi^{\mathrm{T}}(s)\psi(s)\right\} \leq \epsilon_3, \quad \forall s \in [\bar{\sigma},0)_{\mathbb{Z}}, \tag{16}$$

where $\psi(k) = e(k+1) - e(k)$ is the relative error and ϵ_3 is a given positive constant. According to the right inequation in Definition 1, $\psi(k)$ definitely satisfies $\mathcal{E}\left\{\psi^{\mathrm{T}}(s)\psi(s)\right\} \leq \partial$. If there is a constant $\epsilon_3 \geq \partial$, in equation (16) holds.

Lemma 1[31] For the initial value $\Gamma_i(0) \geq 0, \forall i \in N$, the in equation $\eta_i\Gamma_i(k) + \delta_i e_i^{\mathrm{T}}(k)e_i(k) - \varepsilon_i^{\mathrm{T}}(k)\varepsilon_i(k) \geq 0$ can hold always if the selected parameters satisfy $\eta_i\hat{\rho}_i \geq 1$ with $\eta_i \in (0,1)$ and $\hat{\rho}_i > 0$ for $i \in N$.

Lemma 2[22] For a real scalar $o \in (0,1)$, two symmetric matrices $\mathcal{S}_1 > 0$, $\mathcal{S}_2 > 0$, and any matrices $\mathcal{W}_1$, $\mathcal{W}_2$, the following form of ERCMI exists:

$$\begin{aligned}&\begin{bmatrix} \frac{1}{o}\mathcal{S}_1 & 0 \\ 0 & \frac{1}{1-o}\mathcal{S}_2 \end{bmatrix} \\ &\geq \begin{bmatrix} \mathcal{S}_1 + (1-o)\aleph_1 & (1-o)\mathcal{W}_1 + o\mathcal{W}_2 \\ * & \mathcal{S}_2 + o\aleph_2 \end{bmatrix},\end{aligned} \tag{17}$$

where $\aleph_1 = \mathcal{S}_1 - \mathcal{W}_2\mathcal{S}_2^{-1}\mathcal{W}_2^{\mathrm{T}}$ and $\aleph_2 = \mathcal{S}_2 - \mathcal{W}_1^{\mathrm{T}}\mathcal{S}_1^{-1}\mathcal{W}_1$.

Lemma 3[41] For a positive matrix $\mathcal{Q}$ and positive integer $\nu_1 < \nu_2$, any discrete-time variable $\chi(k) \in \mathbb{R}^n$ can satisfy the following inequality:

$$\begin{aligned}&\sum_{i=\nu_1}^{\nu_2-1} \varsigma^{\mathrm{T}}(i)\mathcal{Q}\varsigma(i) \\ &\geq \frac{1}{\nu_2-\nu_1}\begin{bmatrix}\Im_1 \\ \Im_2\end{bmatrix}^{\mathrm{T}}\begin{bmatrix}\mathcal{Q} & 0 \\ * & 3\left(1+\frac{2}{\nu_2-\nu_1-1}\right)\mathcal{Q}\end{bmatrix}\begin{bmatrix}\Im_1 \\ \Im_2\end{bmatrix},\end{aligned} \tag{18}$$

where $\varsigma(k) = \chi(k+1) - \chi(k)$, $\Im_1 = \chi(\nu_2) - \chi(\nu_1)$ and $\Im_2 = \chi(\nu_2) + \chi(\nu_1) - 2\sum_{i=\nu_1}^{\nu_2} \frac{\chi(i)}{\nu_2-\nu_1+1}$.

3. Main results

In this section, the finite-time strictly dissipative synchronization conditions are discussed and the desired controller is designed under the DDETM.

3.1. Finite-time boundness analysis

The finite-time boundness of synchronization errors will be analyzed firstly in the following theorem. Consider the semi-Markov switched error system (13) affected by random packet losses.

Theorem 1 Suppose that conditions (A_1)–(A_3) hold, $\eta_i \in (0,1)$, $\hat{\rho}_i > 0$ with $\eta_i\hat{\rho}_i \geq 1$ for $i = 1,2,\ldots N$ and controller gain is provided. For given $0 < \epsilon_1 < \epsilon_2$, ϵ_3, $\tilde{\rho}_i$, $\underline{\sigma}$, $\bar{\sigma}$, $\underline{\tau}$, $\bar{\tau}$ and $\tilde{\omega}$, the error system (13) achieves finite-time boundness with respect to $(\epsilon_1, \epsilon_2, \mathcal{X}, \mathcal{T}, \tilde{\omega})$ if there is the existence of positive definite matrices $\mathcal{P}_{1,s} = \mathrm{diag}\{\mathcal{P}_{11,s}, \mathcal{P}_{12,s}, \mathcal{P}_{13,s}\}$, $\mathcal{P}_2 = \mathrm{diag}\{\mathcal{P}_{21}, \mathcal{P}_{22}\}$, $\mathcal{W}$, $\mathcal{R}$, $\mathcal{Q}$, $\mathcal{U} = \mathrm{diag}\{\mathcal{U}_1, \mathcal{U}_2\}$, $\mathcal{H}$, symmetric matrices M_1, M_2, any matrices Θ_1, Θ_2, positive diagonal matrices $\Re_1$, $\Re_2$, and positive scalar c_j $(j = 0,1,\ldots,10)$ satisfying the following LMIs for $\forall s \in \mathcal{V}$ and $\forall \ell \in \mathcal{L}$:

$$\begin{aligned}&\mathcal{P}_{s,[\underline{\sigma}]}^{\dagger} > 0, \quad \mathcal{P}_{s,[\bar{\sigma}]}^{\dagger} > 0, \\ &\begin{bmatrix} R_{[\underline{\tau},\underline{\sigma}]}^{m,v,s,\ell} & \Xi_{[\underline{\sigma},\sigma(k)]}\Theta_2 \\ * & -\xi^{-\underline{\sigma}-1}\beth_2 \end{bmatrix} < 0, \quad \begin{bmatrix} R_{[\underline{\tau},\bar{\sigma}]}^{m,v,s,\ell} & \Xi_{[\sigma(k),\bar{\sigma}]}\Theta_1^{\mathrm{T}} \\ * & -\xi^{-\underline{\sigma}-1}\beth_1 \end{bmatrix} < 0, \\ &\begin{bmatrix} R_{[\bar{\tau},\underline{\sigma}]}^{m,v,s,\ell} & \Xi_{[\underline{\sigma},\sigma(k)]}\Theta_2 \\ * & -\xi^{-\underline{\sigma}-1}\beth_2 \end{bmatrix} < 0, \quad \begin{bmatrix} R_{[\bar{\tau},\bar{\sigma}]}^{m,v,s,\ell} & \Xi_{[\sigma(k),\bar{\sigma}]}\Theta_1^{\mathrm{T}} \\ * & -\xi^{-\underline{\sigma}-1}\beth_1 \end{bmatrix} < 0, \\ &c_0\mathcal{X} \leq \mathcal{P}_{11,s} \leq c_1\mathcal{X}, \quad \mathcal{P}_{1j,s} \leq c_j\mathcal{X}, \quad j = 2,3, \\ &\mathcal{P}_{2j} \leq c_{j+3}\mathcal{X}, \quad j = 1,2, \\ &\mathcal{W} \leq c_6\mathcal{X}, \quad \mathcal{R} \leq c_7\mathcal{X}, \quad \mathcal{Q} \leq c_8 I, \\ &\mathcal{U}_1 \leq c_9\mathcal{X}, \quad \mathcal{U}_2 \leq c_{10}I, \\ &\zeta_1\epsilon_1 + \zeta_2\epsilon_3 + \zeta_3 + c_{\max}(\mathcal{H})\tilde{\omega} \leq \xi^{-\mathcal{T}}c_{11}\epsilon_2,\end{aligned} \tag{19}$$

where

$$\begin{aligned}\mathcal{P}_{s,[\sigma(k)]}^{\dagger} &= \mathcal{P}_{1,s} + \sigma\begin{bmatrix}\mathcal{P}_2 & 0 \\ * & 0\end{bmatrix}, \quad \tilde{\mathcal{P}}_{1,s}^{l} = \sum\nolimits_{t\in\mathcal{V}} \mu_\ell \psi_{st}^{\ell}\mathcal{P}_{1,t}, \\ R_{[\tau(k),\sigma(k)]}^{m,v,s,\ell} &= \Pi_{1,[\sigma(k)]}^{m,v,s,\ell} + \Pi_{2,[\tau(k),\sigma(k)]}^{m,v,s,\ell} + \sigma^2(\Omega_2^{m,v})^{\mathrm{T}}\mathcal{Q}\Omega_2^{m,v} \\ &\quad + \sum_{i=1}^{6}\Lambda_i + \Lambda_{[\sigma(k)]}, \\ \Pi_{1,[\sigma(k)]}^{m,v,s,\ell} &= (\nabla_2^{m,v})^{\mathrm{T}}\tilde{\mathcal{P}}_{1,s}^{l}\nabla_2^{m,v} - \nabla_3^{\mathrm{T}}\mathcal{P}_{1,s}\nabla_3 \\ &\quad + \sigma\mathrm{Sym}\left\{\nabla_1^{\mathrm{T}}\tilde{\mathcal{P}}_{1,s}^{l}\nabla_2^{m,v} - \nabla_1^{\mathrm{T}}\mathcal{P}_{1,s}\nabla_3\right\}, \\ \Pi_{2,[\tau(k),\sigma(k)]}^{m,v,s,\ell} &= \tau(\nabla_4^{m,v})^{\mathrm{T}}\mathcal{P}_2\nabla_4^{m,v} \\ &\quad + \sigma\left[(\nabla_4^{m,v})^{\mathrm{T}}\mathcal{P}_2\nabla_4^{m,v} - \nabla_5^{\mathrm{T}}\mathcal{P}_2\nabla_5\right], \\ \nabla_1 &= \left[0,0,\mathcal{I}_7^{\mathrm{T}} - \mathcal{I}_8^{\mathrm{T}}\right]^{\mathrm{T}}, \\ \nabla_4^{m,v} &= \left[(\Omega_1^{m,v})^{\mathrm{T}}, (\underline{\sigma}+1)\mathcal{I}_7^{\mathrm{T}} - \mathcal{I}_2^{\mathrm{T}}\right]^{\mathrm{T}}, \\ \nabla_2^{m,v} &= \left[(\Omega_1^{m,v})^{\mathrm{T}}, (1+\underline{\sigma})\mathcal{I}_7^{\mathrm{T}} - \mathcal{I}_1^{\mathrm{T}}, (1-\underline{\sigma})\mathcal{I}_8^{\mathrm{T}}\right. \\ &\quad \left. + (\bar{\sigma}+1)\mathcal{I}_9^{\mathrm{T}} - \mathcal{I}_3^{\mathrm{T}} - \mathcal{I}_4^{\mathrm{T}}\right]^{\mathrm{T}}, \\ \nabla_3 &= \left[\mathcal{I}_1^{\mathrm{T}}, (1+\sigma)\mathcal{I}_7^{\mathrm{T}} - \mathcal{I}_1^{\mathrm{T}}, (1-\underline{\sigma})\mathcal{I}_8^{\mathrm{T}}\right. \\ &\quad \left. + (\bar{\sigma}+1)\mathcal{I}_9^{\mathrm{T}} - \mathcal{I}_2^{\mathrm{T}} - \mathcal{I}_3^{\mathrm{T}}\right]^{\mathrm{T}}, \\ \nabla_5 &= \left[\mathcal{I}_1^{\mathrm{T}}, (\underline{\sigma}+1)\mathcal{I}_7^{\mathrm{T}} - \mathcal{I}_1^{\mathrm{T}}\right], \\ \Omega_1^{m,v} &= \left[\boldsymbol{A}_m^s - \boldsymbol{R}_m^s\mathcal{K}_v^s\Sigma(k) + G^s\otimes L, 0,0,0,\right. \\ &\quad \boldsymbol{B}_m^s, \boldsymbol{D}_m^s, 0,0,0, \boldsymbol{R}_m^s\mathcal{K}_v^s(I-\Sigma(k)), \\ &\quad \left.\boldsymbol{O}_m^s, \boldsymbol{R}_m^s\mathcal{K}_v^s\Sigma(k), 0\right]^{\mathrm{T}}, \\ \Omega_2^{m,v} &= \left[\boldsymbol{A}_m^s - \boldsymbol{R}_m^s\mathcal{K}_v^s\Sigma(k) + G^s\otimes L - I, 0,0,0,\right. \\ &\quad \boldsymbol{B}_m^s, \boldsymbol{D}_m^s, 0,0,0, \boldsymbol{R}_m^s\mathcal{K}_v^s(I-\Sigma(k)), \boldsymbol{O}_m^s, \\ &\quad \left.\boldsymbol{R}_m^s\mathcal{K}_v^s\Sigma(k), 0\right]^{\mathrm{T}}, \\ \Lambda_1 &= \mathcal{I}_1^{\mathrm{T}}\Sigma^{\mathrm{T}}(k)\mathcal{W}\Sigma(k)\mathcal{I}_1 + \mathcal{I}_{12}^{\mathrm{T}}\Sigma^{\mathrm{T}}(k)\mathcal{W}\Sigma(k)\mathcal{I}_{12} \\ &\quad + \mathcal{I}_{10}^{\mathrm{T}}(I-\Sigma(k))^{\mathrm{T}}\mathcal{W}(I-\Sigma(k))\mathcal{I}_{10} \\ &\quad + \mathrm{Sym}\left\{\mathcal{I}_1^{\mathrm{T}}\Sigma^{\mathrm{T}}(k)\mathcal{W}(I-\Sigma(k))\mathcal{I}_{10}\right. \\ &\quad \left. - \mathcal{I}_1^{\mathrm{T}}\Sigma^{\mathrm{T}}(k)\mathcal{W}\Sigma(k)\mathcal{I}_{12} - \mathcal{I}_{12}^{\mathrm{T}}\Sigma^{\mathrm{T}}(k)\mathcal{W}\right.\end{aligned}$$

$$
\begin{aligned}
&\times (I-\Sigma(k))\mathcal{I}_{10}\big\}-\xi\mathcal{I}_{10}^{\mathrm{T}}\mathcal{W}\mathcal{I}_{10},\\
\Lambda_2 &= (\bar{\sigma}-\underline{\sigma}+1)\mathcal{I}_1^{\mathrm{T}}\mathcal{R}\mathcal{I}_1-\xi^{\bar{\sigma}}\mathcal{I}_3^{\mathrm{T}}\mathcal{R}\mathcal{I}_3,\\
\Lambda_3 &= \phi_1^{\mathrm{T}}\begin{bmatrix}\mathcal{Q} & 0\\ * & 3\mathcal{Q}(\underline{\sigma}+1)/(\underline{\sigma}-1)\end{bmatrix}\phi_1,\\
\Lambda_4 &= \Delta_\sigma^2\phi_2^{\mathrm{T}}\mathcal{U}\phi_2-\xi^{\sigma+1}\Delta_\sigma(\mathcal{I}_2^{\mathrm{T}}M_1\mathcal{I}_2-\mathcal{I}_4^{\mathrm{T}}M_2\mathcal{I}_4\\
&\quad -\mathcal{I}_3^{\mathrm{T}}M_1\mathcal{I}_3+\mathcal{I}_3^{\mathrm{T}}M_2\mathcal{I}_3),\\
\Lambda_5 &= \phi_3^{\mathrm{T}}\begin{bmatrix}-\mathcal{A}_1\mathfrak{R}_1 & \mathcal{A}_2\mathfrak{R}_1\\ * & -\mathfrak{R}_1\end{bmatrix}\phi_3\\
&\quad +\phi_4^{\mathrm{T}}\begin{bmatrix}-\mathcal{B}_1\mathfrak{R}_2 & \mathcal{B}_2\mathfrak{R}_2\\ * & -\mathfrak{R}_2\end{bmatrix}\phi_4,\\
\Lambda_6 &= \mathcal{I}_1^{\mathrm{T}}\mathrm{diag}_N\left\{\xi^{-1}\frac{\delta_i}{\hat{\rho}_i}+\hbar\delta_i\right\}\mathcal{I}_1\\
&\quad -\mathcal{I}_{12}^{\mathrm{T}}\mathrm{diag}_N\left\{\frac{\xi^{-1}}{\hat{\rho}_i}+\hbar\right\}\mathcal{I}_{12}\\
&\quad +\mathcal{I}_{13}^{\mathrm{T}}\mathrm{diag}_N\left\{\frac{\xi^{-1}\eta_i-1+\hbar}{\hat{\rho}_i}\right\}\mathcal{I}_{13},\\
\Lambda_{[\underline{\sigma}]} &= -\phi_5^{\mathrm{T}}\begin{bmatrix}2_1 & \aleph_1\\ * & 2\end{bmatrix}\phi_5,\quad \Lambda_{[\bar{\sigma}]}=-\phi_5^{\mathrm{T}}\begin{bmatrix}1 & \aleph_2\\ * & 2_2\end{bmatrix}\phi_5,\\
\beth_s &= \mathcal{U}+\begin{bmatrix}0 & M_s\\ * & M_s\end{bmatrix},\quad s=1,2,\\
\phi_5 &= \left[\Xi_{[\sigma,\sigma(k)]}^{\mathrm{T}},\Xi_{[\sigma(k),\bar{\sigma}]}^{\mathrm{T}}\right]^{\mathrm{T}},\\
\phi_1 &= \begin{bmatrix}\mathcal{I}_1-\mathcal{I}_2\\ \mathcal{I}_1+\mathcal{I}_2-2\mathcal{I}_7\end{bmatrix},\quad \phi_2=\begin{bmatrix}\mathcal{I}_1\\ \Omega_2^{m,v}\end{bmatrix},\\
\phi_3 &= \begin{bmatrix}\mathcal{I}_1\\ \mathcal{I}_5\end{bmatrix},\quad \phi_4=\begin{bmatrix}\mathcal{I}_3\\ \mathcal{I}_6\end{bmatrix},\\
\Xi_{[\sigma,\sigma(k)]} &= \begin{bmatrix}\mathcal{I}_8\\ \mathcal{I}_2-\mathcal{I}_3\end{bmatrix},\quad \Xi_{[\sigma(k),\bar{\sigma}]}=\begin{bmatrix}\mathcal{I}_9\\ \mathcal{I}_3-\mathcal{I}_4\end{bmatrix},\\
\mathcal{I}_i &= \left[0_{nN\times(i-1)nN},I_{nN},0_{nN\times(13-i)nN}\right],\\
&\quad i=1,2,\ldots,13,\\
\mathcal{A}_1 &= I_N\otimes\tilde{\mathcal{A}}_1,\quad \mathcal{A}_2=I_N\otimes\tilde{\mathcal{A}}_2,\\
\mathcal{B}_1 &= I_N\otimes\tilde{\mathcal{B}}_1,\quad \mathcal{B}_2=I_N\otimes\tilde{\mathcal{B}}_2,\\
\tilde{\mathcal{A}}_1 &= \mathrm{diag}_n\left\{\alpha_l^-\alpha_l^+\right\},\quad \tilde{\mathcal{A}}_2=\frac{1}{2}\mathrm{diag}_n\left\{\alpha_l^-+\alpha_l^+\right\},\\
\tilde{\mathcal{B}}_1 &= \mathrm{diag}_n\left\{\beta_l^-\beta_l^+\right\},\quad \tilde{\mathcal{B}}_2=\frac{1}{2}\mathrm{diag}_n\left\{\beta_l^-+\beta_l^+\right\},\\
\zeta_1 &= c_1+c_2\underline{\sigma}^2+c_3\Delta_\sigma^2+c_4+c_5\underline{\sigma}^2+c_6+\bar{\sigma}\xi^{\bar{\sigma}-1}c_7\\
&\quad +0.5\Delta_\sigma(\bar{\sigma}+\underline{\sigma}-1)\xi^{\bar{\sigma}-2}c_7\\
&\quad +0.5\Delta_\sigma^2(\bar{\sigma}+\underline{\sigma}+1)\xi^{\bar{\sigma}-1}c_9,\\
\zeta_2 &= 0.5\big[\bar{\sigma}^2(\bar{\sigma}+1)\xi^{\sigma-1}c_8\\
&\quad +\Delta_\sigma^2(\bar{\sigma}+\underline{\sigma}+1)\xi^{\bar{\sigma}-1}c_{10}\big],\\
\zeta_3 &= \sum_{i=1}^{N}\xi^{-1}\frac{\Gamma_i^0}{\hat{\rho}_i}.
\end{aligned}
\tag{20}
$$

Proof For $k\in[k_i^q,k_i^{q+1})$ and any $\lambda(k)\in\mathcal{V}$, an augmented mode-dependent LKF candidate is established as follows:

$$
V(k,\lambda(k))=\sum_{i=1}^{6}V_i(k,\lambda(k)),
\tag{21}
$$

where

$$
\begin{aligned}
V_1(k,\lambda(k)) &= \varpi_1^{\mathrm{T}}(k)\mathcal{P}_{1,\lambda(k)}\varpi_1(k)+\sigma\varpi_2^{\mathrm{T}}(k)\mathcal{P}_2\varpi_2(k),\\
V_2(k,\lambda(k)) &= \bar{e}^{\mathrm{T}}(k-1)\mathcal{W}\bar{e}(k-1),\\
V_3(k,\lambda(k)) &= \sum_{i=1}^{N}\xi^{-1}\frac{1}{\hat{\rho}_i}\Gamma_i(k),\\
V_4(k,\lambda(k)) &= \sum_{\vartheta=k-\sigma}^{k-1}\xi^{k-\vartheta-1}e^{\mathrm{T}}(\vartheta)\mathcal{R}e(\vartheta)\\
&\quad +\sum_{l=k-\bar{\sigma}+1}^{k-\sigma}\sum_{\vartheta=l}^{k-1}\xi^{k-\vartheta-1}e^{\mathrm{T}}(\vartheta)\mathcal{R}e(\vartheta),\\
V_5(k,\lambda(k)) &= \sigma\sum_{l=k-\sigma}^{k-1}\sum_{\vartheta=l}^{k-1}\xi^{k-\vartheta-1}\psi^{\mathrm{T}}(\vartheta)\mathcal{Q}\psi(\vartheta),\\
V_6(k,\lambda(k)) &= \Delta_\sigma\sum_{l=k-\bar{\sigma}}^{k-\sigma-1}\sum_{\vartheta=l}^{k-1}\xi^{k-\vartheta-1}\varpi_3^{\mathrm{T}}(\vartheta)\mathcal{U}\varpi_3(\vartheta),
\end{aligned}
$$

where

$$
\begin{aligned}
\varpi_1(k) &= [e^{\mathrm{T}}(k),\textstyle\sum_{\vartheta=k-\underline{\sigma}}^{k-1}e^{\mathrm{T}}(\vartheta),\sum_{\vartheta=k-\bar{\sigma}}^{k-\sigma-1}e^{\mathrm{T}}(\vartheta)]^{\mathrm{T}},\\
\varpi_2(k) &= [e^{\mathrm{T}}(k),\textstyle\sum_{\vartheta=k-\underline{\sigma}}^{k-1}e^{\mathrm{T}}(\vartheta)],\\
\varpi_3(k) &= [e^{\mathrm{T}}(k),\psi^{\mathrm{T}}(k)]^{\mathrm{T}}.
\end{aligned}
$$

Define $\Delta V(k,\lambda(k))=V(k+1,\lambda(k+1))-\xi V(k,\lambda(k))$, we can obtain $\mathcal{E}\{\Delta V(k,\lambda(k))\}$ along the trajectories of the error system (13), and it follows that

$$
\begin{aligned}
&\mathcal{E}\{\Delta V_1(k,\lambda(k))\}\\
&= \mathcal{E}\Big\{\varpi_1^{\mathrm{T}}(k+1)\sum_{t\in\mathcal{V}}\psi_{st}(k)\mathcal{P}_{1,t}\varpi_1(k+1)-\xi\varpi_1^{\mathrm{T}}(k)\mathcal{P}_{1,s}\varpi_1(k)\\
&\quad +\sigma(k+1)\varpi_2^{\mathrm{T}}(k+1)\mathcal{P}_2\varpi_2(k+1)-\xi\sigma\varpi_2^{\mathrm{T}}(k)\mathcal{P}_2\varpi_2(k)\Big\}\\
&\le \mathcal{E}\Big\{\sum_{m=1}^{r}\sum_{v=1}^{r}\Im_m\Im_v\wp^{\mathrm{T}}(k)\big[(\sigma\nabla_1+\nabla_2^m)^{\mathrm{T}}\tilde{\mathcal{P}}_{1,s}(\sigma\nabla_1+\nabla_2^m)\\
&\quad -\xi(\sigma\nabla_1+\nabla_3)^{\mathrm{T}}\mathcal{P}_{1,s}(\sigma\nabla_1+\nabla_3)+(\tau+\sigma)\\
&\quad \times(\nabla_4^m)^{\mathrm{T}}\mathcal{P}_2\nabla_4^m-\sigma\nabla_5^{\mathrm{T}}\mathcal{P}_2\nabla_5\big]\wp(k),
\end{aligned}
\tag{22}
$$

where $\tilde{\mathcal{P}}_s=\sum_{\ell\in\mathcal{L}}\sum_{t\in\mathcal{V}}\mu_\ell\psi_{st}^\ell\mathcal{P}_t$ and

$$
\begin{aligned}
\wp(k) &= \Big[e^{\mathrm{T}}(k),e^{\mathrm{T}}(k-\underline{\sigma}),e^{\mathrm{T}}(k-\sigma),e^{\mathrm{T}}(k-\bar{\sigma}),F^{\mathrm{T}}(e(k)),\\
&\quad H^{\mathrm{T}}(e(k-\sigma)),\textstyle\sum_{\vartheta=k-\sigma}^{k}e^{\mathrm{T}}(\vartheta),\sum_{\vartheta=k-\sigma}^{k-\sigma}e^{\mathrm{T}}(\vartheta),\\
&\quad \textstyle\sum_{\vartheta=k-\bar{\sigma}}^{k-\sigma}e^{\mathrm{T}}(\vartheta),\bar{e}^{\mathrm{T}}(k-1),\omega^{\mathrm{T}}(k)\varepsilon^{\mathrm{T}}(k),\Gamma^{1/2}(k)\Big]^{\mathrm{T}}.
\end{aligned}
$$

$$
\begin{aligned}
&\mathcal{E}\{\Delta V_2(k,\lambda(k))\}\\
&= \mathcal{E}\left\{\bar{e}^{\mathrm{T}}(k)\mathcal{W}\bar{e}(k)-\xi\bar{e}^{\mathrm{T}}(k-1)\mathcal{W}\bar{e}(k-1)\right\}\\
&= \mathcal{E}\big\{e^{\mathrm{T}}(k)\Sigma^{\mathrm{T}}(k)\mathcal{W}\Sigma(k)e(k)+\varepsilon^{\mathrm{T}}(k)\Sigma^{\mathrm{T}}(k)\mathcal{W}\Sigma(k)\varepsilon(k)\\
&\quad +\bar{e}^{\mathrm{T}}(k-1)(I-\Sigma(k))^{\mathrm{T}}\mathcal{W}(I-\Sigma(k))\bar{e}(k-1)\\
&\quad +\mathrm{Sym}\big\{e^{\mathrm{T}}(k)\Sigma^{\mathrm{T}}(k)\mathcal{W}(I-\Sigma(k))\bar{e}(k-1)-e^{\mathrm{T}}(k)\\
&\quad \times\Sigma^{\mathrm{T}}(k)\mathcal{W}\Sigma(k)\varepsilon(k)-\varepsilon^{\mathrm{T}}(k)\Sigma^{\mathrm{T}}(k)\mathcal{W}(I-\Sigma(k))\bar{e}(k-1)\big\}\\
&\quad -\xi\bar{e}^{\mathrm{T}}(k-1)\mathcal{W}\bar{e}(k-1)\big\}\\
&= \mathcal{E}\left\{\wp^{\mathrm{T}}(k)\Lambda_1\wp(k)\right\}.
\end{aligned}
\tag{23}
$$

$$
\begin{aligned}
&\mathcal{E}\{\Delta V_3(k,\lambda(k))\}\\
&=\mathcal{E}\Big\{\sum_{i=1}^{N}\xi^{-1}\frac{1}{\hat{\rho}_i}(\eta_i\Gamma_i(k)+\delta_i e_i^{\mathrm{T}}(k)e_i(k)\\
&\quad-\varepsilon_i^{\mathrm{T}}(k)\varepsilon_i(k))-\sum_{i=1}^{N}\frac{1}{\hat{\rho}_i}\Gamma_i(k)\Big\}\\
&=\mathcal{E}\Big\{\sum_{i=1}^{N}\frac{1}{\hat{\rho}_i}\Gamma_i(k)(\xi^{-1}\eta_i-1)+\sum_{i=1}^{N}\xi^{-1}\frac{\delta_i}{\hat{\rho}_i}e_i^{\mathrm{T}}(k)e_i(k)\\
&\quad-\sum_{i=1}^{N}\xi^{-1}\frac{1}{\hat{\rho}_i}\varepsilon_i^{\mathrm{T}}(k)\varepsilon_i(k)\Big\}. \qquad (24)\\
&\mathcal{E}\{\Delta V_4(k,\lambda(k))\}\\
&\le e^{\mathrm{T}}(k)\mathcal{R}e(k)-\xi^{\bar{\sigma}}e^{\mathrm{T}}(k-\sigma)\mathcal{R}e(k-\sigma)\\
&\quad+\sum_{\vartheta=k+1-\bar{\sigma}}^{k-\underline{\sigma}}\xi^{k-\vartheta}e^{\mathrm{T}}(\vartheta)\mathcal{R}e(\vartheta)\\
&\quad+(\bar{\sigma}-\sigma)e^{\mathrm{T}}(k)\mathcal{R}e(k)-\sum_{\vartheta=k+1-\bar{\sigma}}^{k-\underline{\sigma}}\xi^{k-\vartheta}e^{\mathrm{T}}(\vartheta)\mathcal{R}e(\vartheta)\\
&=\wp^{\mathrm{T}}(k)\Lambda_2\wp(k). \qquad (25)\\
&\mathcal{E}\{\Delta V_5(k,\lambda(k))\}\\
&=\mathcal{E}\Big\{\sigma\sum_{l=k+1-\underline{\sigma}}^{k}\sum_{\vartheta=l}^{k}\xi^{k-\vartheta}\psi^{\mathrm{T}}(\vartheta)\mathcal{Q}\psi(\vartheta)\\
&\quad-\underline{\sigma}\sum_{l=k-\underline{\sigma}}^{k-1}\sum_{\vartheta=l}^{k-1}\xi^{k-\vartheta-1}\psi(\vartheta)\mathcal{Q}\psi(\vartheta)\Big\}\\
&\le\mathcal{E}\Big\{\underline{\sigma}^2\psi^{\mathrm{T}}(k)\mathcal{Q}\psi(k)-\xi\underline{\sigma}\sum_{\vartheta=k-\underline{\sigma}}^{k-1}\psi^{\mathrm{T}}(\vartheta)\mathcal{Q}\psi(\vartheta)\Big\}. \qquad (26)
\end{aligned}
$$

Using Lemma 3, we can obtain

$$
\begin{aligned}
&-\xi\sigma\sum_{\vartheta=k-\underline{\sigma}}^{k-1}\psi^{\mathrm{T}}(\vartheta)\mathcal{Q}\psi(\vartheta)\\
&\le\begin{bmatrix}\phi_{11}\\ \phi_{12}\end{bmatrix}^{\mathrm{T}}\begin{bmatrix}\mathcal{Q} & 0\\ * & 3\mathcal{Q}(\underline{\sigma}+1)/(\underline{\sigma}-1)\end{bmatrix}\begin{bmatrix}\phi_{11}\\ \phi_{12}\end{bmatrix}, \qquad (27)
\end{aligned}
$$

where $\phi_{11}=e(k)-e(k-\underline{\sigma})$, $\phi_{12}=e(k)+e(k-\underline{\sigma})-2\sum_{\vartheta=k-\underline{\sigma}}^{k}e(\vartheta)$. Therefore, expression (25) can be further transformed into

$$
\begin{aligned}
&\mathcal{E}\{\Delta V_5(k,\lambda(k))\}\\
&\le\mathcal{E}\Big\{\sum_{m=1}^{r}\sum_{v=1}^{r}\Im_m\Im_v\big[\underline{\sigma}^2\wp^{\mathrm{T}}(k)(\Omega_2^{m,v})^{\mathrm{T}}\mathcal{Q}\Omega_2^{m,v}\wp(k)\\
&\quad-\wp^{\mathrm{T}}(k)\Lambda_3\wp(k)\big]\Big\}. \qquad (28)
\end{aligned}
$$

Then,

$$
\begin{aligned}
&\mathcal{E}\{\Delta V_6(k,\lambda(k))\}\\
&=\mathcal{E}\Big\{\Delta_\sigma\sum_{l=k+1-\bar{\sigma}}^{k-\underline{\sigma}}\sum_{\vartheta=l}^{k}\xi^{k-\vartheta}\varpi_3^{\mathrm{T}}(\vartheta)\mathcal{U}\varpi_3(\vartheta)\\
&\quad-\Delta_\sigma\sum_{l=k-\bar{\sigma}}^{k-\underline{\sigma}-1}\sum_{\vartheta=l}^{k-1}\xi^{k-\vartheta-1}\varpi_3^{\mathrm{T}}(\vartheta)\mathcal{U}\varpi_3(\vartheta)\Big\}\\
&\le\mathcal{E}\Big\{\Delta_\sigma^2\varpi_3^{\mathrm{T}}(k)\mathcal{U}\varpi_3(k)\\
&\quad-\xi^{\sigma+1}\Delta_\sigma\sum_{\vartheta=k-\bar{\sigma}}^{k-\underline{\sigma}+1}\varpi_3^{\mathrm{T}}(\vartheta)\mathcal{U}\varpi_3(\vartheta)\Big\}. \qquad (29)
\end{aligned}
$$

To estimate the bound of $\mathcal{E}\{\Delta V_5(k,\lambda(k))\}$, the following zero-value equations are presented for any symmetric matrices M_1 and M_2:

$$
\begin{aligned}
0&=\Delta_\sigma e^{\mathrm{T}}(k-\underline{\sigma})M_1e(k-\underline{\sigma})-\Delta_\sigma e^{\mathrm{T}}(k-\sigma)M_1e(k-\sigma)\\
&\quad-\Delta_\sigma\sum_{\vartheta=k-\sigma}^{k-\underline{\sigma}-1}\varpi_3^{\mathrm{T}}(\vartheta)\begin{bmatrix}0 & M_1\\ * & M_1\end{bmatrix}\varpi_3(\vartheta), \qquad (30)\\
0&=\Delta_\sigma e^{\mathrm{T}}(k-\sigma)M_1e(k-\sigma)-\Delta_\sigma e^{\mathrm{T}}(k-\bar{\sigma})M_2e(k-\bar{\sigma})\\
&\quad-\Delta_\sigma\sum_{\vartheta=k-\bar{\sigma}}^{k-\sigma-1}\varpi_3^{\mathrm{T}}(\vartheta)\begin{bmatrix}0 & M_2\\ * & M_2\end{bmatrix}\varpi_3(\vartheta). \qquad (31)
\end{aligned}
$$

With the combination of Eqs. (30) and (31), it follows from Jensen's inequality theory that

$$
\begin{aligned}
&-\Delta_\sigma\sum_{\vartheta=k-\bar{\sigma}}^{k-\sigma-1}\varpi_2^{\mathrm{T}}(\vartheta)\mathcal{U}\varpi_2(\vartheta)\\
&=\Delta_\sigma e^{\mathrm{T}}(k-\underline{\sigma})M_1e(k-\underline{\sigma})-\Delta_\sigma e^{\mathrm{T}}(k-\bar{\sigma})M_2e(k-\bar{\sigma})\\
&\quad-\Delta_\sigma e^{\mathrm{T}}(k-\sigma)(M_1-M_2)e(k-\sigma)\\
&\quad-\Delta_\sigma\sum_{\vartheta=k-\sigma}^{k-\sigma-1}\varpi_3^{\mathrm{T}}(\vartheta)\left(\mathcal{U}+\begin{bmatrix}0 & M_1\\ * & M_1\end{bmatrix}\right)\varpi_3(\vartheta)\\
&\quad-\Delta_\sigma\sum_{\vartheta=k-\sigma}^{k-\sigma-1}\varpi_3^{\mathrm{T}}(\vartheta)\left(\mathcal{U}+\begin{bmatrix}0 & M_2\\ * & M_2\end{bmatrix}\right)\varpi_3(\vartheta)\\
&\le\Delta_\sigma\wp^{\mathrm{T}}(k)(\mathcal{I}_2^{\mathrm{T}}M_1\mathcal{I}_2-\mathcal{I}_4^{\mathrm{T}}M_2\mathcal{I}_4-\mathcal{I}_3^{\mathrm{T}}M_1\mathcal{I}_3+\mathcal{I}_3^{\mathrm{T}}M_2\mathcal{I}_3)\wp(k)\\
&\quad-\wp^{\mathrm{T}}(k)\Pi_{3,[\sigma(k)]}\wp(k), \qquad (32)
\end{aligned}
$$

where the delay-dependent term $\Pi_{3,[\sigma(k)]}$ is described as

$$
\Pi_{3,[\sigma(k)]}=\frac{1}{\upsilon}\Xi_{[\underline{\sigma},\sigma(k)]}^{\mathrm{T}}\beth_1\Xi_{[\underline{\sigma},\sigma(k)]}+\frac{1}{1-\upsilon}\Xi_{[\sigma(k),\bar{\sigma}]}^{\mathrm{T}}\beth_2\Xi_{[\sigma(k),\bar{\sigma}]},
$$

with $\upsilon=(\sigma-\underline{\sigma})/\Delta_\sigma$, and $\Xi_{[\underline{\sigma},\sigma(k)]}$,$\Xi_{[\sigma(k),\bar{\sigma}]}$ are provided in Eq. (20).

Relying on the inequality (17) in Lemma 2, $\Pi_{3,[\sigma(k)]}$ can be further bounded as follows:

$$
\begin{aligned}
&\Pi_{3,[\sigma(k)]}\ge\tilde{\Pi}_{3,[\sigma(k)]}\\
&=\begin{bmatrix}\Xi_{[\underline{\sigma},\sigma(k)]}\\ \Xi_{[\sigma(k),\bar{\sigma}]}\end{bmatrix}^{\mathrm{T}}\begin{bmatrix}\beth_1+(1-\upsilon)\aleph_1 & (1-\upsilon)\Theta_1+\upsilon\Theta_2\\ * & \beth_2+\upsilon\aleph_2\end{bmatrix}\begin{bmatrix}\Xi_{[\underline{\sigma},\sigma(k)]}\\ \Xi_{[\sigma(k),\bar{\sigma}]}\end{bmatrix} \qquad (33)
\end{aligned}
$$

for any matrices Θ_1 and Θ_2, where $\aleph_1=\beth_1-\Theta_2\beth_2^{-1}\Theta_2^{\mathrm{T}}$ and $\aleph_2=\beth_2-\Theta_1^{\mathrm{T}}\beth_1^{-1}\Theta_1$. Thus,

$$
\begin{aligned}
&\mathcal{E}\{\Delta V_5(k,\lambda(k))\}\\
&\le\mathcal{E}\Big\{\wp^{\mathrm{T}}(k)\sum_{m=1}^{r}\sum_{v=1}^{r}\Im_m\Im_v\big[\Delta_\sigma^2(\phi_2^{m,v})^{\mathrm{T}}\mathcal{U}\phi_2^{m,v}\\
&\quad-\xi^{\sigma+1}\Delta_\sigma(\mathcal{I}_2^{\mathrm{T}}M_1\mathcal{I}_2-\mathcal{I}_4^{\mathrm{T}}M_2\mathcal{I}_4-\mathcal{I}_3^{\mathrm{T}}M_1\mathcal{I}_3\\
&\quad+\mathcal{I}_3^{\mathrm{T}}M_2\mathcal{I}_3)-\xi^{\underline{\sigma}+1}\tilde{\Pi}_{3,[\sigma(k)]}\big]\wp(k)\\
&=\mathcal{E}\Big\{\wp^{\mathrm{T}}(k)\sum_{m=1}^{r}\sum_{v=1}^{r}\Im_m\Im_v(\Lambda_4-\xi^{\underline{\sigma}+1}\tilde{\Pi}_{3,[\sigma(k)]})\wp(k)\Big\}. \qquad (34)
\end{aligned}
$$

Notice that activation functions satisfy the Lipschitz continuity in (A_2), and one has the following inequations:

$$0 \leq \begin{bmatrix} e(k) \\ F(e(k)) \end{bmatrix}^{\mathrm{T}} \begin{bmatrix} -\mathcal{A}_1\Re_1 & \mathcal{A}_2\Re_1 \\ * & -\Re_1 \end{bmatrix} \begin{bmatrix} e(k) \\ F(e(k)) \end{bmatrix}, \tag{35}$$

$$0 \leq \begin{bmatrix} e(k-\sigma) \\ H(e(k-\sigma)) \end{bmatrix}^{\mathrm{T}} \begin{bmatrix} -\mathcal{B}_1\Re_2 & \mathcal{B}_2\Re_2 \\ * & -\Re_2 \end{bmatrix} \begin{bmatrix} e(k-\sigma) \\ H(e(k-\sigma)) \end{bmatrix}, \tag{36}$$

where $\mathcal{A}_1$, $\mathcal{A}_2$, $\mathcal{B}_1$ and $\mathcal{B}_2$ are defined in Eq. (20). Moreover, based on the event-triggered constraint condition (8), we can derive that for any positive constant $\hbar$,

$$\begin{aligned} 0 &\geq \hbar \left(\sum_{i=1}^{N} Q(e_i(k), \delta_i) - \sum_{i=1}^{N} \frac{\Gamma_i(k)}{\hat{\rho}_i} \right), \\ 0 &\geq \hbar \left(\sum_{i=1}^{N} \varepsilon_i^{\mathrm{T}}(k)\varepsilon_i(k) - \sum_{i=1}^{N} \delta_i e_i^{\mathrm{T}}(k)e_i(k) - \sum_{i=1}^{N} \frac{\Gamma_i(k)}{\hat{\rho}_i} \right). \end{aligned} \tag{37}$$

Repeating the process from inequations (21)–(35), we easily get

$$\begin{aligned} &\mathcal{E}\left\{\Delta V(k,\lambda(k)) - \omega^{\mathrm{T}}(k)\mathcal{H}\omega(k)\right\} \\ &\leq \mathcal{E}\left\{ \sum_{m=1}^{r}\sum_{v=1}^{r} \Im_m \Im_v \wp^{\mathrm{T}}(k) \Psi^{m,v,s,\ell}_{[\tau(k),\sigma(k)]} \wp(k) \right\}, \end{aligned} \tag{38}$$

where

$$\begin{aligned} &\Psi^{m,v,s,\ell}_{[\tau(k),\sigma(k)]} \\ &= \sum_{\ell\in\mathcal{L}} \mu_\ell \Big\{ (\sigma\nabla_1 + \nabla_2^m)^{\mathrm{T}} \\ &\quad \times \sum_{t\in\mathcal{V}} \psi_{st}^{\ell} \mathcal{P}_{1,s}(\sigma\nabla_1 + \nabla_2^m) - \xi(\sigma\nabla_1 + \nabla_3)^{\mathrm{T}} \\ &\quad \times \mathcal{P}_{1,s}(\sigma\nabla_1 + \nabla_3) + (\tau+\sigma)(\nabla_4^m)^{\mathrm{T}}\mathcal{P}_2\nabla_4^m - \sigma\nabla_5^{\mathrm{T}}\mathcal{P}_2\nabla_5 \\ &\quad + \Lambda_1 + \Lambda_2 + (\Omega_2^m)^{\mathrm{T}}\mathcal{Q}\Omega_2^m \\ &\quad - \phi_1^{\mathrm{T}}\Lambda_3\phi_1 + \Lambda_4 + \Lambda_5 - \tilde{\Pi}_{3,[\sigma(k)]} \Big\} \\ &= \sum_{\ell\in\mathcal{L}} \mathrm{F}_\ell \left\{ R^{m,v,s,\ell}_{[\tau(k),\sigma(k)]} + \tilde{\Pi}_{3,[\sigma(k)]} \right\} \end{aligned} \tag{39}$$

and $R^{m,v,s,\ell}_{[\tau(k),\sigma(k)]}$ is stated in Eq. (20). From the convex combination technique and (A_1), we have the following inference:

$$\begin{cases} \Psi^{m,v,s,\ell}_{[\underline{\tau},\underline{\sigma}]} < 0, \Psi^{m,v,s,\ell}_{[\underline{\tau},\bar{\sigma}]} < 0 \\ \Psi^{m,v,s,\ell}_{[\bar{\tau},\underline{\sigma}]} < 0, \Psi^{m,v,s,\ell}_{[\bar{\tau},\bar{\sigma}]} < 0 \end{cases} \Rightarrow \Psi^{m,v,s,\ell}_{[\tau(k),\sigma(k)]} < 0. \tag{40}$$

Then, with the help of the Schur complement theory, the constraint $\Psi^{m,v,s,\ell}_{[\sigma]} < 0$ will hold for $\underline{\sigma} \leq \sigma(k) \leq \bar{\sigma}$ if inequation (18) is satisfied, such that

$$\mathcal{E}\left\{\Delta V(k,\lambda(k)) - \omega^{\mathrm{T}}(k)\mathcal{H}\omega(k)\right\} < 0. \tag{41}$$

Hence, we can further conduct the following iterative operation with regard to finite time k:

$$\begin{aligned} &\mathcal{E}\{V(k,\lambda(k))\} \\ &\leq \mathcal{E}\left\{\xi V(k-1,\lambda(k-1)) + \omega^{\mathrm{T}}(k-1)\mathcal{H}\omega(k-1)\right\} \\ &\leq \mathcal{E}\big\{\xi^2 V(k-2,\lambda(k-2)) + \xi\omega^{\mathrm{T}}(k-2)\mathcal{H}\omega(k-2) \\ &\quad + \omega^{\mathrm{T}}(k-1)\mathcal{H}\omega(k-1)\big\} \\ &\quad \vdots \\ &\leq \mathcal{E}\Big\{\xi^k V(0,\lambda(0)) + \sum_{\vartheta=0}^{k-1} \xi^{k-\vartheta-1}\omega^{\mathrm{T}}(\vartheta)\mathcal{H}\omega(\vartheta)\Big\} \\ &\leq \mathcal{E}\left\{\xi^k V(0,\lambda(0)) + c_{\max}(\mathcal{H})\xi^k\tilde{\omega}\right\}, \end{aligned} \tag{42}$$

where $c_{\max}(\mathcal{H})$ is the maximum eigenvalue of matrix $\mathcal{H}$. The value of $V(0,\lambda(0))$ is estimated as

$$\begin{aligned} &\mathcal{E}\{V(0,\lambda(0))\} \\ &= \mathcal{E}\left\{\varpi_1^{\mathrm{T}}(0)\mathcal{P}_{1,s}\varpi_1(0) + \varpi_1^{\mathrm{T}}(0)\mathcal{P}_2\varpi_1(0)\right\} \\ &\quad + \mathcal{E}\left\{\bar{e}^{\mathrm{T}}(-1)\mathcal{W}\bar{e}(-1)\right\} + \mathcal{E}\left\{\sum_{i=1}^{N} \xi^{-1}\frac{1}{\hat{\rho}_i}\Gamma_i(0)\right\} \\ &\quad + \mathcal{E}\Bigg\{\sum_{\vartheta=-\sigma(0)}^{-1} \xi^{-\vartheta-1}e^{\mathrm{T}}(\vartheta)\mathcal{R}e(\vartheta) \\ &\quad + \sum_{l=-\bar{\sigma}+1}^{-\sigma}\sum_{\vartheta=l}^{-1} \xi^{-\vartheta-1}e^{\mathrm{T}}(\vartheta)\mathcal{R}e(\vartheta)\Bigg\} \\ &\quad + \mathcal{E}\left\{\underline{\sigma}\sum_{l=k-\underline{\sigma}}^{k-1}\sum_{\vartheta=l}^{k-1} \xi^{k-\vartheta-1}\psi^{\mathrm{T}}(\vartheta)\mathcal{Q}\psi(\vartheta)\right\} \\ &\quad + \mathcal{E}\left\{\Delta_\sigma \sum_{l=-\bar{\sigma}}^{-\sigma-1}\sum_{\vartheta=l}^{-1} \xi^{-\vartheta-1}\varpi_2^{\mathrm{T}}(\vartheta)\mathcal{U}\varpi_2(\vartheta)\right\} \\ &\leq \zeta_1\epsilon_1 + \zeta_2\epsilon_3 + \zeta_3. \end{aligned} \tag{43}$$

With the combination of inequations (42) and (43), we have

$$\mathcal{E}\{V(k,\lambda(k))\} \leq \xi^{\mathcal{T}}(\zeta_1\epsilon_1 + \zeta_2\epsilon_3 + \zeta_3 + c_{\max}(\mathcal{H})\tilde{\omega}). \tag{44}$$

Due to the condition $\mathcal{P}_{11,s} \geq c_{11}\mathcal{X}$ in Eq. (19), it exists as

$$\begin{aligned} &\mathcal{E}\{V(k,\lambda(k))\} \\ &\geq \mathcal{E}\left\{e^{\mathrm{T}}(k)\mathcal{P}_{11,s}e(k)\right\} \geq c_{11}\mathcal{E}\left\{e^{\mathrm{T}}(k)\mathcal{X}e(k)\right\}, \end{aligned} \tag{45}$$

such that the following inequation holds:

$$\begin{aligned} &\mathcal{E}\left\{e^{\mathrm{T}}(k)\mathcal{X}e(k)\right\} \\ &\leq \frac{\xi^{\mathcal{T}}}{c_{11}}(\zeta_1\epsilon_1 + \zeta_2\epsilon_3 + \zeta_3 + c_{\max}(\mathcal{H})\tilde{\omega}) \leq \epsilon_2. \end{aligned} \tag{46}$$

The finite-time boundness of the error system (13) can be eventually derived. This completes the proof. □

Remark 4 In the finite-time boundness analysis of the closed-loop error system, an augmented mode-dependent LKF, containing vectors $\varpi_1(k)$, $\varpi_2(k)$ and $\varpi_3(k)$, is constructed and inspired by Ref. [23]. Differing from the common LKF that is only formed by error or state vectors, the augmented terms observe more information of delays through more sum-terms. Specifically, the improved delay-product-type terms in $V_1(k,\lambda(k))$ and $V_6(k,\lambda(k))$ further consider the change rate of $\sigma(k)$ and develop the results in Ref. [41]. Moreover, the proposed $\mathcal{P}^{\dagger}_{s,[\sigma(k)]} > 0$ in Eq. (19) provides a more relaxed range for the stability criterion.

Remark 5 In Refs. [11,27,31], some inequality techniques, such as Abel lemma, Wirtinger-based inequality and Jensen's inequality, were introduced to handle the single sum-term or simple double sum-term. However, the delay-product-type double sum term in $V_6(k,\lambda(k))$ will contribute to more nonlinearities and uncertainty. To obtain more accurate estimation, the ERCMI is raised by not introducing additional decision variables or adding the dimension of LMIs, in order to further reduce the conservatism.

3.2. Finite-time strict dissipativity analysis

In this subsection, both the sufficient criterion of the dissipative FTS for closed-loop TSFCPSs and the design of the related fuzzy controller gain $K_{i,v}^{\lambda(k)}$ are given.

Theorem 2 Suppose that conditions (A$_1$)–(A$_3$) hold, $\eta_i \in (0,1)$, $\hat{\rho}_i > 0$ with $\eta_i\hat{\rho}_i \geq 1$ for $i = 1,2,\ldots N$. For given $0 < \epsilon_1 < \epsilon_2$, ϵ_3, $\tilde{\rho}_i$, $\underline{\sigma}$, $\bar{\sigma}$, $\underline{\tau}$, $\bar{\tau}$, the real matrices $\Upsilon_1 = \Upsilon_1^{\mathrm{T}} \leq 0$, Υ_2, $\Upsilon_3 = \Upsilon_3^{\mathrm{T}}$ and the diagonal matrix $\tilde{L}$, the closed-loop system (1) is said to be FTS with strict dissipativity if there is the existence of the constant $\tilde{\gamma} > 0$, positive definite matrices $\mathcal{P}_{1,s}$, $\mathcal{P}_2$, $\mathcal{W}$, $\mathcal{R}$, $\mathcal{Q}$, $\mathcal{U}$, symmetric matrices M_1, M_2, any matrices Θ_1, Θ_2, positive diagonal matrices $\Re_1$, $\Re_2$, matrices $\mathcal{F}_v^s = \mathrm{diag}_N\left\{\mathcal{F}_{i,v}^s\right\}$, $\mathcal{M}_v^s = \mathrm{diag}_N\left\{\mathcal{M}_{i,v}^s\right\}$ and positive scalar c_j $(j = 0,1,\ldots,10)$, such that the following conditions are met for $\forall s \in \mathcal{V}$ and $\forall \ell \in \mathcal{L}$:

$$
\begin{aligned}
&\mathcal{P}_{[\underline{\sigma}]}^{\dagger} > 0, \quad \mathcal{P}_{[\bar{\sigma}]}^{\dagger} > 0,\\
&\begin{bmatrix} \tilde{R}_{[\underline{\tau},\underline{\sigma}]}^{m,v,s,\ell} & \Xi_{[\underline{\sigma},\sigma(k)]}\Theta_2 \\ * & -\xi^{-\underline{\sigma}-1}\beth_2 \end{bmatrix} < 0, \quad \begin{bmatrix} \tilde{R}_{[\underline{\tau},\bar{\sigma}]}^{m,v,s,\ell} & \Xi_{[\sigma(k),\bar{\sigma}]}\Theta_1^{\mathrm{T}} \\ * & -\xi^{-\underline{\sigma}-1}\beth_1 \end{bmatrix} < 0,\\
&\begin{bmatrix} \tilde{R}_{[\bar{\tau},\underline{\sigma}]}^{m,v,s,\ell} & \Xi_{[\underline{\sigma},\sigma(k)]}\Theta_2 \\ * & -\xi^{-\underline{\sigma}-1}\beth_2 \end{bmatrix} < 0, \quad \begin{bmatrix} \tilde{R}_{[\bar{\tau},\bar{\sigma}]}^{m,v,s,\ell} & \Xi_{[\sigma(k),\bar{\sigma}]}\Theta_1^{\mathrm{T}} \\ * & -\xi^{-\underline{\sigma}-1}\beth_1 \end{bmatrix} < 0,\\
&c_0\mathcal{X} \leq \mathcal{P}_{11,s} \leq c_1\mathcal{X}, \quad \mathcal{P}_{1j,s} \leq c_j\mathcal{X}, \quad j = 2,3,\\
&\mathcal{P}_{2j} \leq c_{j+3}\mathcal{X}, \quad j = 1,2,\\
&\mathcal{W} \leq c_6\mathcal{X}, \quad \mathcal{R} \leq c_7\mathcal{X}, \quad \mathcal{Q} \leq c_8 I,\\
&\mathcal{U}_1 \leq c_9\mathcal{X}, \quad \mathcal{U}_2 \leq c_{10} I,\\
&\zeta_1\epsilon_1 + \zeta_2\epsilon_3 + \zeta_3 + c_{\max}(\mathcal{H})\tilde{\omega} \leq \xi^{-\mathcal{T}}c_{11}\epsilon_2,
\end{aligned} \tag{47}
$$

where

$$
\begin{aligned}
\tilde{R}_{[\tau(k),\sigma(k)]}^{m,v,s,\ell} &= \Pi_{1,[\sigma(k)]}^{m,v,s,\ell} + \Pi_{2,[\tau(k),\sigma(k)]}^{m,v,s,\ell} + \underline{\sigma}^2(\tilde{\Omega}_2^{m,v})^{\mathrm{T}}\mathcal{Q}\tilde{\Omega}_2^{m,v}\\
&\quad + (\tilde{\Omega}_1^{m,v})^{\mathrm{T}}\mathcal{F}_v^s\tilde{\Omega}_1^{m,v} + \sum_{i=1}^{7}\Lambda_i + \Lambda_8^m + \Lambda_{[\sigma(k)]},\\
\tilde{\Omega}_1^{m,v} &= \big[\boldsymbol{A}_m^s - (\mathcal{F}_v^s)^{-1}\mathcal{M}_v^s\Sigma(k)\\
&\quad + G^s\otimes L, 0,0,0, \boldsymbol{B}_m^s, \boldsymbol{D}_m^s, 0,0,0,\\
&\quad (\mathcal{F}_v^s)^{-1}\mathcal{M}_v^s(I-\Sigma(k)), \boldsymbol{O}_m^s, (\mathcal{F}_v^s)^{-1}\mathcal{M}_v^s\Sigma(k), 0\big]^{\mathrm{T}},\\
\tilde{\Omega}_2^{m,v} &= \big[\boldsymbol{A}_m^s - (\mathcal{F}_v^s)^{-1}\mathcal{M}_v^s\Sigma(k)\\
&\quad + G^s\otimes L - I, 0,0,0, \boldsymbol{B}_m^s, \boldsymbol{D}_m^s, 0,0,0,\\
&\quad (\mathcal{F}_v^s)^{-1}\mathcal{M}_v^s(I-\Sigma(k)), \boldsymbol{O}_m^s, (\mathcal{F}_v^s)^{-1}\mathcal{M}_v^s\Sigma(k), 0\big]^{\mathrm{T}},
\end{aligned}
$$

$$
\begin{aligned}
\Lambda_7 &= \mathrm{Sym}\big\{-(\Omega_1^{m,v})^{\mathrm{T}}\mathcal{F}_v^s(\boldsymbol{A}_m^s\mathcal{I}_1 + \boldsymbol{B}_m^s\mathcal{I}_5 + \boldsymbol{D}_m^s\mathcal{I}_6\\
&\quad + \boldsymbol{O}_m^s\mathcal{I}_{11}) + (\Omega_1^{m,v})^{\mathrm{T}}\mathcal{M}_v^s\\
&\quad \times\big[\boldsymbol{L}\Sigma(k)\mathcal{I}_1 - \boldsymbol{L}\Sigma(k)\mathcal{I}_{12} + \boldsymbol{L}(I-\Sigma(k))\mathcal{I}_{10}\big]\\
&\quad - (\Omega_1^{m,v})^{\mathrm{T}}(G^s\otimes L)\mathcal{I}_1\big\},\\
\Lambda_8^m &= \mathcal{I}_1^{\mathrm{T}}(\boldsymbol{C}_m^s)^{\mathrm{T}}\Upsilon_1\boldsymbol{C}_m^s\mathcal{I}_1 + Sym\big\{\mathcal{I}_1^{\mathrm{T}}(\boldsymbol{C}_m^s)^{\mathrm{T}}\Upsilon_1\boldsymbol{E}_m^s\mathcal{I}_{11}\big\}\\
&\quad + \mathcal{I}_{11}^{\mathrm{T}}(\boldsymbol{E}_m^s)^{\mathrm{T}}\Upsilon_1\boldsymbol{E}_m^s\mathcal{I}_{11}\\
&\quad + \mathrm{Sym}\big\{\mathcal{I}_1^{\mathrm{T}}(\boldsymbol{C}_m^s)^{\mathrm{T}}\Upsilon_2\mathcal{I}_{11} + \mathcal{I}_{11}^{\mathrm{T}}(\boldsymbol{E}_m^s)^{\mathrm{T}}\Upsilon_2\mathcal{I}_{11}\big\}\\
&\quad + \mathcal{I}_{11}^{\mathrm{T}}(\Upsilon_3 - \tilde{\gamma}I)\mathcal{I}_{11},
\end{aligned} \tag{48}
$$

and other parameters are defined in Eq. (20). Moreover, the controller gain matrix is described as

$$
K_{i,v}^s = (R_m^s)^{-1}(\mathcal{F}_{i,v}^s)^{-1}\mathcal{M}_{i,v}^s, \quad i = 1,2,\ldots N, \quad s \in \mathcal{V}.
$$

Proof Considering the LKF candidate constructed in Theorem 1. For any invertible matrix $\mathcal{F}_v^s$, one has the following zero-value equation:

$$
\begin{aligned}
0 \leq\ & 2\sum_{m=1}^{r}\sum_{v=1}^{r}\Im_m\Im_v\big\{e^{\mathrm{T}}(k_1)\mathcal{F}_v^s\big[e(k+1) - (\boldsymbol{A}_m^s - \boldsymbol{R}_m^s\mathcal{K}_v^s\Sigma(k)\\
&+ G^s\otimes L)e(k) - \boldsymbol{B}_m^sF(e(k)) - \boldsymbol{D}_m^sH(e(k-\sigma)) - \boldsymbol{O}_m^s\omega(k)\\
&- \boldsymbol{R}_m^s\mathcal{K}_v^s\Sigma(k)\varepsilon(k) + \boldsymbol{R}_m^s\mathcal{K}_v^s(I-\Sigma(k))\bar{e}(k-1)\big]\big\}\\
\leq\ & 2\sum_{m=1}^{r}\sum_{v=1}^{r}\Im_m\Im_v\wp^{\mathrm{T}}(k)\big\{(\Omega_1^{m,v})^{\mathrm{T}}\\
&\times\big[\mathcal{F}_v^s\Omega_1^{m,v} - \mathcal{F}_v^s\mathcal{A}_m^s\mathcal{I}_1 + \mathcal{M}_v^s\Sigma(k)\mathcal{I}_1\\
&- G^s\otimes L\mathcal{I}_1 - \mathcal{F}_v^s\boldsymbol{B}_m^s\mathcal{I}_5 - \mathcal{F}_v^s\boldsymbol{D}_m^s\mathcal{I}_6 - \mathcal{F}_v^s\boldsymbol{O}_m^s\mathcal{I}_{11}\\
&- \mathcal{M}_v^s\Sigma(k)\mathcal{I}_{12} + \mathcal{M}_v^s(I-\Sigma(k))\mathcal{I}_{10}\big]\big\}\wp(k).
\end{aligned} \tag{49}
$$

As the controller is greatly impacted by the pinning parameter φ_i, we can further obtain the following inequation:

$$
\begin{aligned}
0 \leq\ & 2\sum_{m=1}^{r}\sum_{v=1}^{r}\Im_m\Im_v\wp^{\mathrm{T}}(k)\big\{(\Omega_1^{m,v})^{\mathrm{T}}\\
&\times\big[\mathcal{F}_v^s\Omega_1^{m,v} - \mathcal{F}_v^s\boldsymbol{A}_m^s\mathcal{I}_1 + \mathcal{M}_v^s\mathcal{L}\Sigma(k)\mathcal{I}_1\\
&- (G^s\otimes L)\mathcal{I}_1 - \mathcal{F}_v^s\boldsymbol{B}_m^s\mathcal{I}_5 - \mathcal{F}_v^s\boldsymbol{D}_m^s\mathcal{I}_6 - \mathcal{F}_v^s\boldsymbol{O}_m^s\mathcal{I}_{11}\\
&- \mathcal{M}_v^s\mathcal{L}\Sigma(k)\mathcal{I}_{12} + \mathcal{M}_v^s\tilde{L}(I-\Sigma(k))\mathcal{I}_{10}\big]\big\}\wp(k),
\end{aligned} \tag{50}
$$

where $\tilde{L} = \mathrm{diag}_N\{\tilde{L}_i\}$, $\tilde{L}_i = I_n$ if the ith node is controlled, otherwise $\tilde{L}_i = 0_n$.

To study the strictly dissipative performance of the synchronization error system, an object function is constructed as follows:

$$
\begin{aligned}
G(k) &= e_y^{\mathrm{T}}(k)\Upsilon_1e_y(k) + 2e_y^{\mathrm{T}}(k)\Upsilon_2\omega(k)\\
&\quad + \omega^{\mathrm{T}}(k)(\Upsilon_3 - \tilde{\gamma}I)\omega(k).
\end{aligned} \tag{51}
$$

Similar to Eq. (38), it derives from Eqs. (49)–(51) that

$$
\begin{aligned}
&\mathcal{E}\{\Delta V(k,\lambda(k)) - G(k)\}\\
&\leq \mathcal{E}\left\{\sum_{m=1}^{r}\sum_{v=1}^{r}\Im_m\Im_v\wp^{\mathrm{T}}(k)\tilde{\Psi}_{[\tau(k),\sigma(k)]}^{m,v,s,\ell}\wp(k)\right\}.
\end{aligned} \tag{52}
$$

where $\tilde{\Psi}_{[\tau(k),\sigma(k)]}^{m,v,s,\ell} = \sum_{\ell\in\mathcal{L}}\mu_\ell\left\{\tilde{R}_{[\tau(k),\sigma(k)]}^{m,v,s,\ell} + \tilde{\Pi}_{3,[\sigma(k)]}\right\}$ and $\tilde{R}_{[\tau(k),\sigma(k)]}^{m,v,s,\ell}$ is defined in Eq. (48).

Recalling Eq. (40) and the application of the Schur complement, we can get $\mathcal{E}\{\Delta V(k,\lambda(k))-G(k)\}\leq 0$, which is equivalent to

$$\mathcal{E}\{V(k+1,\lambda(k+1))\}\leq \mathcal{E}\{\xi V(k,\lambda(k))+G(k)\}.$$

Based on the iterative operation within the time interval $[0,k]$ in Eq. (42), it derives the following inequation under the zero-initial condition:

$$\begin{aligned}
&\mathcal{E}\{V(k,\lambda(k))\}\\
&\leq \mathcal{E}\Big\{\xi^{k}V(0,\lambda(0))-\sum_{\vartheta=0}^{k-1}\xi^{k-\vartheta-1}\mathcal{J}(e_y(\vartheta),\omega(\vartheta))\\
&\quad+\tilde{\gamma}\sum_{\vartheta=0}^{k-1}\xi^{k-\vartheta-1}\omega^{\mathrm{T}}(\vartheta)\omega(\vartheta)\Big\}\\
&\leq \mathcal{E}\Big\{\xi^{\mathcal{T}}\tilde{\gamma}\sum_{\vartheta=0}^{k-1}\omega^{\mathrm{T}}(\vartheta)\omega(\vartheta)-\sum_{\vartheta=0}^{k-1}\mathcal{J}(e(\vartheta),\omega(\vartheta))\Big\}. \quad (53)
\end{aligned}$$

With the premises of $\mathcal{E}\{V(k,\lambda(k))\}>0$, it is easily concluded that

$$\begin{aligned}
&\mathcal{E}\left\{\sum_{k=0}^{\mathcal{T}}\mathcal{J}(e(k),\omega(k))\right\}\leq \mathcal{E}\left\{\gamma\sum_{k=0}^{\mathcal{T}}\omega^{\mathrm{T}}(\vartheta)\omega(\vartheta)\right\},\\
&\gamma=\xi^{\mathcal{T}}\tilde{\gamma}. \quad (54)
\end{aligned}$$

Obviously, the closed-loop TSFCPSs can satisfy finite-time strictly $(\Upsilon_1,\Upsilon_2,\Upsilon_3)$–$\gamma$–dissipative performance in the right of Definition 2. The proof is accomplished. □

Remark 6 In terms of the dissipativeness definition and results of Theorem 1, a new framework is established to analyze the finite-time dissipative synchronization of the closed-loop system, in order to obtain the sufficient condition in Theorem 2. By utilizing the LMI technique, controller gain matrices under various modes can be calculated. Notice that the number of modes and nodes affects complexity; therefore, a tradeoff between computational burden and conservation is necessary in real application.

The following corollary is formulated for the Markov switched CPSs absent from the T-S fuzzy model:

Corollary 1 Suppose that conditions (A_1)–(A_2) hold, $\eta_i\in(0,1)$, $\hat{\rho}_i>0$ with $\eta_i\hat{\rho}_i\geq 1$ for $i=1,2,\ldots N$. For given $0<\epsilon_1<\epsilon_2$, ϵ_3, $\tilde{\rho}_i$, $\underline{\sigma}$, $\bar{\sigma}$, $\underline{\tau}$, $\bar{\tau}$, $\tilde{\omega}$, the real matrices $\Upsilon_1=\Upsilon_1^{\mathrm{T}}\leq 0$, Υ_2, $\Upsilon_3=\Upsilon_3^{\mathrm{T}}$ and the diagonal matrix $\tilde{L}$, the closed-loop system (1) is said to be FTS with strict dissipativity if there is the existence of the constant $\tilde{\gamma}>0$, positive definite matrices $\mathcal{P}_{1,s}$, $\mathcal{P}_2$, $\mathcal{W}$, $\mathcal{R}$, $\mathcal{Q}$, $\mathcal{U}$, symmetric matrices M_1, M_2, any matrices Θ_1, Θ_2, positive diagonal matrices $\Re_1$, $\Re_2$, and positive scalar c_j $(j=0,1,\ldots,10)$, such that the following conditions are meet for $\forall s\in\mathcal{V}$ and $\forall\ell\in\mathcal{L}$:

$$\begin{aligned}
&\mathcal{P}^{\dagger}_{[\underline{\sigma}]}>0,\quad \mathcal{P}^{\dagger}_{[\bar{\sigma}]}>0,\\
&\begin{bmatrix}\widehat{R}^{s,\ell}_{[\underline{\tau},\underline{\sigma}]} & \Xi_{[\underline{\sigma},\sigma(k)]}\Theta_2\\ * & -\xi^{-\underline{\sigma}-1}\beth_2\end{bmatrix}<0,\quad \begin{bmatrix}\widehat{R}^{s,\ell}_{[\underline{\tau},\bar{\sigma}]} & \Xi_{[\sigma(k),\bar{\sigma}]}\Theta_1^{\mathrm{T}}\\ * & -\xi^{-\underline{\sigma}-1}\beth_1\end{bmatrix}<0,\\
&\begin{bmatrix}\widehat{R}^{s,\ell}_{[\bar{\tau},\underline{\sigma}]} & \Xi_{[\underline{\sigma},\sigma(k)]}\Theta_2\\ * & -\xi^{-\underline{\sigma}-1}\beth_2\end{bmatrix}<0,\quad \begin{bmatrix}\widehat{R}^{s,\ell}_{[\bar{\tau},\bar{\sigma}]} & \Xi_{[\sigma(k),\bar{\sigma}]}\Theta_1^{\mathrm{T}}\\ * & -\xi^{-\underline{\sigma}-1}\beth_1\end{bmatrix}<0,\\
&c_0\mathcal{X}\leq\mathcal{P}_{11,s}\leq c_1\mathcal{X},\quad \mathcal{P}_{1j,s}\leq c_j\mathcal{X}\quad(j=2,3),\\
&\mathcal{P}_{2j}\leq c_{j+3}\mathcal{X}\quad(j=1,2),\\
&\mathcal{W}\leq c_6\mathcal{X},\quad \mathcal{R}\leq c_7\mathcal{X},\quad \mathcal{Q}\leq c_8 I,\\
&\mathcal{U}_1\leq c_9\mathcal{X},\quad \mathcal{U}_2\leq c_{10}I,\\
&\zeta_1\epsilon_1+\zeta_2\epsilon_3+\zeta_3+c_{\max}(\mathcal{H})\tilde{\omega}\leq\xi^{-\mathcal{T}}c_{11}\epsilon_2, \quad (55)
\end{aligned}$$

where

$$\begin{aligned}
\widehat{\mathcal{P}}^{\dagger}_{s,[\sigma(k)]} &= \widehat{\mathcal{P}}_{1,s}+\sigma\begin{bmatrix}\mathcal{P}_2 & 0\\ * & 0\end{bmatrix},\quad \widehat{\mathcal{P}}_{1,s}=\textstyle\sum_{t\in\mathcal{V}}\psi_{st}\mathcal{P}_{1,t},\\
\widehat{R}^{s}_{[\tau(k),\sigma(k)]} &= \widehat{\Pi}^{s}_{1,[\sigma(k)]}+\widehat{\Pi}^{s}_{2,[\tau(k),\sigma(k)]}+\widehat{\Omega}_1^{\mathrm{T}}\mathcal{F}^s\widehat{\Omega}_1\\
&\quad+\sigma^2\widehat{\Omega}_2^{\mathrm{T}}\mathcal{Q}\widehat{\Omega}_2+\sum_{i=1}^{8}\Lambda_i+\Lambda_{[\sigma(k)]},\\
\widehat{\Pi}^{s}_{1,[\sigma(k)]} &= \widehat{\nabla}_2^{\mathrm{T}}\widehat{\mathcal{P}}_{1,s}\widehat{\nabla}_2-\nabla_3^{\mathrm{T}}\mathcal{P}_{1,s}\nabla_3\\
&\quad+\sigma\mathrm{Sym}\left\{\nabla_1^{\mathrm{T}}\widehat{\mathcal{P}}_{1,s}\widehat{\nabla}_2-\nabla_1^{\mathrm{T}}\mathcal{P}_{1,s}\nabla_3\right\},\\
\widehat{\Pi}^{s}_{2,[\tau(k),\sigma(k)]} &= \tau\widehat{\nabla}_4^{\mathrm{T}}\mathcal{P}_2\widehat{\nabla}_4+\sigma(\widehat{\nabla}_4^{\mathrm{T}}\mathcal{P}_2\widehat{\nabla}_4-\nabla_5^{\mathrm{T}}\mathcal{P}_2\nabla_5),\\
\widehat{\nabla}_2 &= \big[\widehat{\Omega}_1^{\mathrm{T}},(1+\sigma)\mathcal{I}_7^{\mathrm{T}}-\mathcal{I}_1^{\mathrm{T}},\\
&\quad(1-\sigma)\mathcal{I}_8^{\mathrm{T}}+(\bar{\sigma}+1)\mathcal{I}_9^{\mathrm{T}}-\mathcal{I}_3^{\mathrm{T}}-\mathcal{I}_4^{\mathrm{T}}\big]^{\mathrm{T}},\\
\nabla_4 &= \left[\widehat{\Omega}_1^{\mathrm{T}},(\sigma+1)\mathcal{I}_7^{\mathrm{T}}-\mathcal{I}_2^{\mathrm{T}}\right]^{\mathrm{T}},\quad \phi_2=\left[\mathcal{I}_1^{\mathrm{T}},\widehat{\Omega}_2^{\mathrm{T}}\right]^{\mathrm{T}},\\
\Lambda_8 &= \mathcal{I}_1^{\mathrm{T}}(\boldsymbol{C}^s)^{\mathrm{T}}\Upsilon_1\boldsymbol{C}^s\mathcal{I}_1+\mathrm{Sym}\left\{\mathcal{I}_1^{\mathrm{T}}(\boldsymbol{C}^s)^{\mathrm{T}}\Upsilon_1\boldsymbol{E}^s\mathcal{I}_{11}\right\}\\
&\quad+\mathcal{I}_{11}^{\mathrm{T}}(\boldsymbol{E}^s)^{\mathrm{T}}\Upsilon_1\boldsymbol{E}^s\mathcal{I}_{11}\\
&\quad+\mathrm{Sym}\left\{\mathcal{I}_1^{\mathrm{T}}(\boldsymbol{C}^s)^{\mathrm{T}}\Upsilon_2\mathcal{I}_{11}+\mathcal{I}_{11}^{\mathrm{T}}(\boldsymbol{E}^s)^{\mathrm{T}}\Upsilon_2\mathcal{I}_{11}\right\}\\
&\quad+\mathcal{I}_{11}^{\mathrm{T}}(\Upsilon_3-\tilde{\gamma}I)\mathcal{I}_{11},\\
\widehat{\Omega}_1 &= \big[\boldsymbol{A}^s-(\mathcal{F}^s)^{-1}\mathcal{M}^s\Sigma(k)\\
&\quad+G^s\otimes L,0,0,0,\boldsymbol{B}^s,\boldsymbol{D}^s,0,0,0,\\
&\quad(\mathcal{F}^s)^{-1}\mathcal{M}^s(I-\Sigma(k)),\boldsymbol{O}^s,(\mathcal{F}^s)^{-1}\mathcal{M}^s\Sigma(k),0\big]^{\mathrm{T}},\\
\widehat{\Omega}_2 &= \big[\boldsymbol{A}^s-(\mathcal{F}^s)^{-1}\mathcal{M}^s\Sigma(k)\\
&\quad+G^s\otimes L-I,0,0,0,\boldsymbol{B}^s,\boldsymbol{D}^s,0,0,0,\\
&\quad(\mathcal{F}^s)^{-1}\mathcal{M}^s(I-\Sigma(k)),\boldsymbol{O}^s,\\
&\quad(\mathcal{F}^s)^{-1}\mathcal{M}^s\Sigma(k),0\big]^{\mathrm{T}}, \quad (56)
\end{aligned}$$

and other notations are given by Eq. (48). If LMIs are feasible, the controller gain is calculated as $K_i^s=(R^s)^{-1}(\mathcal{F}_i^s)^{-1}\mathcal{M}_i^s$. Furthermore, we can also derive the condition of finite-time $\mathcal{H}\infty$ synchronization for CPSs when setting $\Upsilon_1=-1$, $\Upsilon_2=0$ and $\Upsilon_3=\gamma^2+\gamma$.

4. Numerical simulations

In this section, numerical examples and simulation results are presented to demonstrate the effectiveness of the proposed theories.

Example 1 Consider the following dynamic equation of the gearing connected single-link robot arm as the target model of CPSs:[25,38]

$$\ddot{q}(t) = -\frac{M_{\lambda(k)}g\tilde{L}}{J_{\lambda(k)}}\sin(q(t)) - \frac{D}{J_{\lambda(k)}}\dot{q}(t) + \omega(k), \tag{57}$$

where $q(t)$ and $\dot{q}(t)$ denote the arm angle position and angular velocity. Given parameter $L = 0.5$, $g = 9.81$, $D = 2$. Here, $M_{\lambda(k)}$ and $J_{\lambda(k)}$ are mode-dependent with $M_1 = 1$, $J_1 = 1$, $M_2 = 5$, $J_2 = 5$, $M_3 = 10$ and $J_3 = 10$.

Set $x_{i1}(t) = q_i(t)$ and $x_{i2}(t) = \dot{q}_i(t)$ for CPSs containing six nodes, and Eq. (57) can be discretized by the first-order Euler approximation method with the sampling period $\Delta t = 0.1$ s. Referring to Ref. [38], the CPSs are constructed by a T-S fuzzy model with the following membership functions:

$$\Im_1(x_{i1}(k)) = \begin{cases} \dfrac{\sin(x_{i1}(k)) - \beta x_{i1}(k)}{(1-\beta)x_{i1}(k)}, & x_{i1}(k) \neq 0, \\ 1, & x_{i1}(k) = 0, \end{cases}$$
$$\Im_2(x_{i1}(k)) = 1 - \Im_1(x_{i1}(k)),$$

where $x_{i1}(k) \in (-\pi, \pi)$, $\beta = 10^{-2}/\pi$. System parameters subject to two fuzzy rules and three modes are selected as

Fuzzy rule 1 If $x_{i1}(k)$ is 0 rad, then

$$A_1^{\lambda(k)} = \begin{bmatrix} 1 & \partial\Delta t \\ 0 & 1 - \dfrac{\partial\Delta t D}{J_{\lambda(k)}} \end{bmatrix}, \quad B_1^{\lambda(k)} = \begin{bmatrix} 0 & 0 \\ 0 & \dfrac{-\Delta t M_{\lambda(k)} g L}{J_{\lambda(k)}} \end{bmatrix},$$
$$C_1^{\lambda(k)} = \begin{bmatrix} 1 & 0 \end{bmatrix}, \quad D_1^{\lambda(k)} = \begin{bmatrix} 0 & \Delta t(1-\partial) \\ 0 & \dfrac{-\Delta t(1-\partial)D}{J_{\lambda(k)}} \end{bmatrix},$$
$$O_1^{\lambda(k)} = \begin{bmatrix} 0 \\ \Delta t \end{bmatrix}, \quad R_1^{\lambda(k)} = \begin{bmatrix} 0 \\ \dfrac{\Delta t}{J_{\lambda(k)}} \end{bmatrix}, \quad E_1^{\lambda(k)} = 1.$$

Fuzzy rule 2 If $x_{i1}(k)$ is $-\pi$ or π rad, then

$$A_2^{\lambda(k)} = \begin{bmatrix} 1 & \partial\Delta t \\ 0 & 1 - \dfrac{\partial\Delta t D}{J_{\lambda(k)}} \end{bmatrix}, \quad B_2^{\lambda(k)} = \begin{bmatrix} 0 & 0 \\ 0 & \dfrac{-\beta\Delta t M_{\lambda(k)} g L}{J_{\lambda(k)}} \end{bmatrix},$$
$$C_2^{\lambda(k)} = \begin{bmatrix} 1 & 0 \end{bmatrix}, \quad D_2^{\lambda(k)} = \begin{bmatrix} 0 & \Delta t(1-\partial) \\ 0 & \dfrac{-\Delta t(1-\partial)D}{J_{\lambda(k)}} \end{bmatrix},$$
$$O_2^{\lambda(k)} = \begin{bmatrix} 0 \\ \Delta t \end{bmatrix}, \quad R_1^{\lambda(k)} = \begin{bmatrix} 0 \\ \dfrac{\Delta t}{J_{\lambda(k)}} \end{bmatrix}, \quad E_2^{\lambda(k)} = 1.$$

The retarded coefficient is set as $\partial = 0.9$.

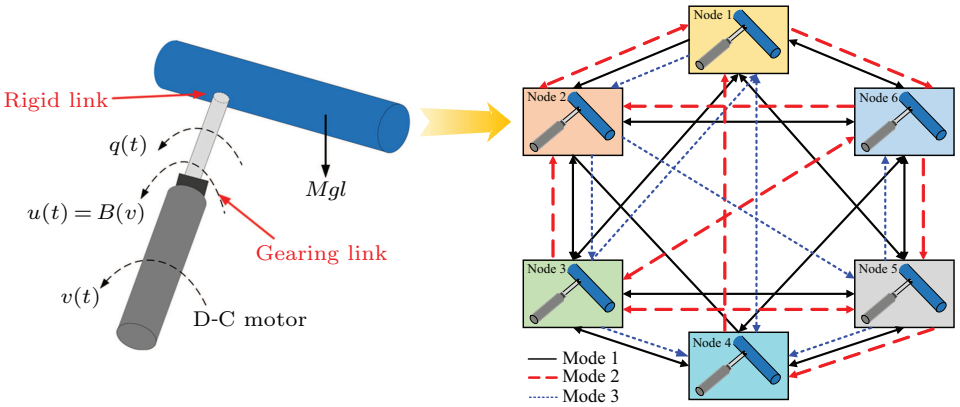


Fig. 3. The physical structure of the gearing connected single-link robot arm and coupled topological relation under three switched modes.

As shown in Fig. 3, CPSs can change topology relations among three modes, and the corresponding elements in the transition probability matrix satisfy

$$\psi_{11} \in [0.3, 0.5], \quad \psi_{22} \in [0.45, 0.65], \quad \psi_{33} \in [0.2, 0.4].$$

When $\mathcal{L} = 2$, the values of ψ_{st}^{ℓ} are given as

$$\begin{aligned}
&\psi_{11}^1 = 0.3, \quad \psi_{12}^1 = 0.4, \quad \psi_{13}^1 = 0.3, \\
&\psi_{11}^2 = 0.4, \quad \psi_{12}^2 = 0.5, \quad \psi_{13}^2 = 0.1, \\
&\psi_{21}^1 = 0.25, \quad \psi_{22}^1 = 0.45, \quad \psi_{23}^1 = 0.3, \\
&\psi_{21}^2 = 0.3, \quad \psi_{22}^2 = 0.5, \quad \psi_{23}^2 = 0.2, \\
&\psi_{31}^1 = 0.3, \quad \psi_{32}^1 = 0.5, \quad \psi_{33}^1 = 0.2, \\
&\psi_{31}^2 = 0.15, \quad \psi_{32}^2 = 0.5, \quad \psi_{33}^2 = 0.35.
\end{aligned}$$

The time-varying delay is set as $\sigma(k) = [3 + 2\sin(\pi k/2)]$ (where $[a]$ means the integer part of a), the disturbance $\omega_i(k) = 2\mathrm{e}^{-0.5k}\sin(k)$. From (A_1) and (A_2), it is easy to get $\underline{\sigma} = 1$, $\bar{\sigma} = 5$, $\underline{\tau} = -2$, $\bar{\tau} = 4$, $\alpha_l^- = \alpha_l^+ = 0$ $(l = 1, 2)$, $\beta_1^- = \beta_1^+ = 0$, $\beta_2^- = \beta_2^+ = 1$.

Assume that nodes 1, 2 and 6 are the controller, some parameters are supposed as $\tilde{L} = \mathrm{diag}\{I, I, 0, 0, 0, I\}$, $\xi = 1.02$, $\epsilon_1 = 10$, $\epsilon_2 = 50$, $\mathcal{T} = 50$, $\tilde{\rho}_1 = \tilde{\rho}_2 = \tilde{\rho}_6 = 0.15$, $\eta_1 = \eta_2 = 0.6$, $\eta_6 = 0.5$, $\hat{\rho}_1 = \hat{\rho}_2 = \hat{\rho}_6 = 25$, $\delta_1 = \delta_2 = \delta_6 = 0.4$ and $\tilde{\omega} = 1.8$. The dissipativity-related matrices are set as $\Upsilon_1 = -0.4I$, $\Upsilon_2 = I$ and $\Upsilon_3 = 4I$. By solving the LMIs proposed in Theorem 2, controller gains and the maximum dissipative level γ are deduced. Table 1 gives the allowable maximum dissipative level γ for different $\bar{\sigma}$ and δ_i, where a larger $\bar{\sigma}$ results in the de-

crease in dissipative level γ and a smaller δ_i will improve the dissipative performance.

Randomly choose the initial values of CPSs within the range of $[-\pi,\pi]$, and let $\tilde{x}(k)=[-3,2]$ for $k\in[-5.0]_{\mathbb{Z}}$. Figure 4 reveals the evolution of synchronization errors under random 200 realizations, which proves that the designed control method can ensure error convergence. As shown in Fig. 5, the states of CPSs subject to packet losses track the state of the target node in finite time $\mathcal{T}$. As Remark 3 said, the PDC method is used and the curves of the controller states and their triggering instants are depicted in Figs. 6(a) and 6(b). The update frequency of the control signals is reduced efficiently.

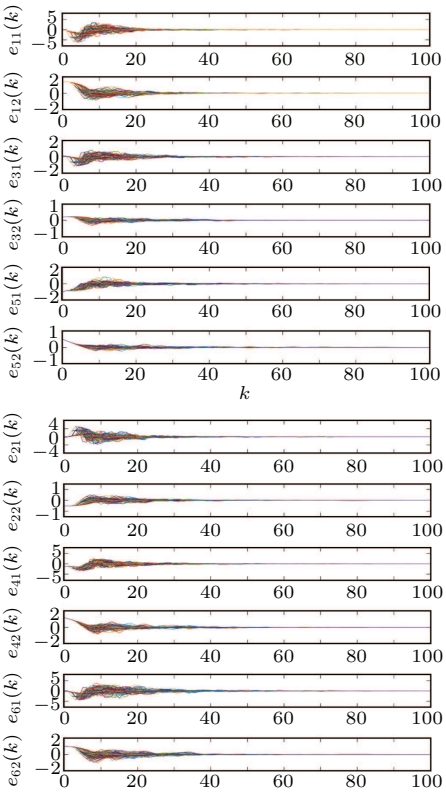


Fig. 4. The response of the synchronization errors in closed-loop CPSs under 200 realizations.

Table 1. The allowable maximum dissipative level γ for various $\bar{\sigma}$ and δ_i.

Maximum values of γ	$\delta_i=0$	$\delta_i=0.2$	$\delta_i=0.4$	$\delta_i=0.6$
$\bar{\sigma}=5$	2.1304	2.1042	1.8646	1.7751
$\bar{\sigma}=8$	2.1531	2.0892	1.8297	1.7110
$\bar{\sigma}=10$	2.0843	2.0092	1.8109	1.6782
$\bar{\sigma}=15$	1.9738	1.9698	1.7287	1.5805

Table 2. A comparison of TR under various methods.

Methods		Node1	Node2	Node6	ATR
DDETM	$\hat{\rho}_i=8$	25%	22%	26%	24.33%
	$\hat{\rho}_i=25$	34%	26%	31%	30.33%
	$\hat{\rho}_i=60$	43%	46%	44%	43.33%
ETM in Ref. [27]		54%	53%	48%	51.67%
ETM in Ref. [28]		100%	100%	100%	100%

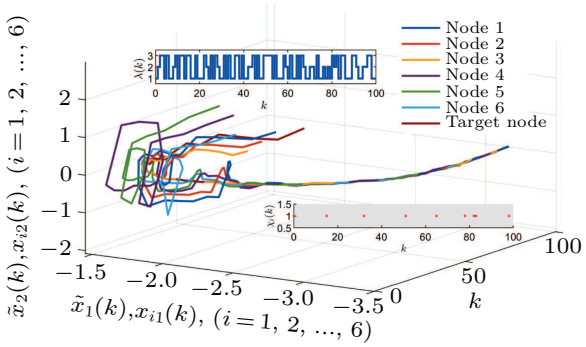


Fig. 5. States of the closed-loop CPSs under packet losses and switched system modes.

To indicate the advantage, Table 2 compares the triggering rate (TR) of three pinned nodes under various triggering mechanisms in Refs. [27,28] and this paper. Clearly, the average TR (ATR) of our used DDETM is significantly lower than techniques in others. Moreover, we observe ATR rises with the growth of $\hat{\rho}_i$.

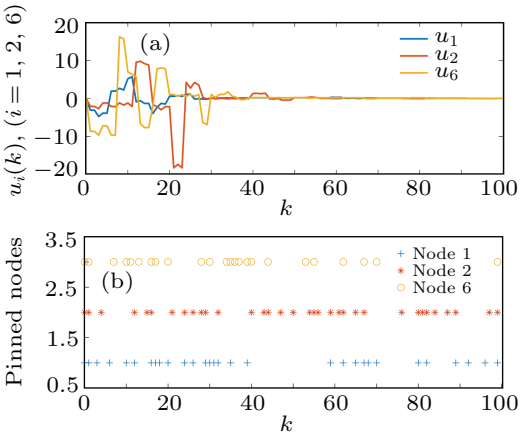


Fig. 6. (a) The curves of controller signals. (b) The triggering instants of controllers 1, 2 and 6.

Example 2 For Corollary 1, consider the Markov double-mode-switched CPSs, including five subsystems where the parameter matrices are provided in Table 3.

Assume that $\sigma(k)=[(3\mathrm{e}^{0.1k}/3\mathrm{e}^{0.1k})+22]$ and $\omega_i(k)=\mathrm{e}^{-0.5k}\sin(k)$, such that $\bar{\sigma}=25$, $\underline{\tau}=0$, $\bar{\tau}=1,\alpha_l^-=\beta_l^-=0$ and $\alpha_l^+=\beta_l^+=1$ for $l=1,2$. With the initial value of $\tilde{x}(0)=[-0.5,0.4]$, the chaotic trajectories of the target system for two modes are plotted in Fig. 7.

Select some parameters as $\tilde{L}=\mathrm{diag}\{I,I,0,0,I\}$, $\xi=1.01$, $\epsilon_1=2$, $\epsilon_2=35$, $\mathcal{T}=150$, $\tilde{\omega}=2$, $\tilde{\rho}_i=0.2$, $\eta_i=0.5$, $\hat{\rho}_1=30$, $\delta_i=0.6$, $\Upsilon_1=-0.15I$, $\Upsilon_2=I$,$\Upsilon_3=2I$. The transition probability matrix and inner coupled matrix are set as

$$\psi=\begin{bmatrix}0.6 & 0.4\\ 0.5 & 0.5\end{bmatrix},\quad G^s=\begin{bmatrix}-0.4 & 0.1 & 0.1 & 0.1 & 0.1\\ 0.2 & -0.4 & 0.1 & 0.1 & 0.1\\ 0.1 & 0.2 & -0.6 & 0.1 & 0.2\\ 0.1 & 0.1 & 0 & -0.3 & 0.1\\ 0.2 & 0.1 & 0.1 & 0 & -0.4\end{bmatrix}.$$

Based on LMIs given in Eq. (55), we can calculate the

feasible controller gains as follows:

$$K_1^1 = \begin{bmatrix} -92.4926 & 59.3270 \\ 51.1689 & 19.1023 \end{bmatrix}, \quad K_1^2 = \begin{bmatrix} -92.8342 & 59.0177 \\ 52.2130 & 19.7529 \end{bmatrix},$$

$$K_2^1 = \begin{bmatrix} -85.5660 & 41.0672 \\ 50.6870 & 20.0815 \end{bmatrix}, \quad K_2^2 = \begin{bmatrix} -85.2175 & 41.8210 \\ 50.8136 & 20.1023 \end{bmatrix},$$

$$K_5^1 = \begin{bmatrix} -25.2617 & 12.4900 \\ 21.5129 & 10.1137 \end{bmatrix}, \quad K_5^2 = \begin{bmatrix} -25.3299 & 13.0365 \\ 21.7782 & 10.6318 \end{bmatrix},$$

and the allowable maximum dissipative level $\gamma = 2.5261$.

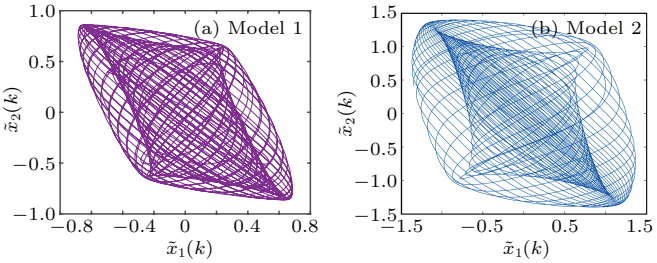


Fig. 7. The phase diagram of $\tilde{x}(k)$ for two switched modes.

Table 3. System parameter matrices for each mode.

Mode	A	B	D	R	O	C	E
1	$\begin{bmatrix} 0.85 & 0 \\ 0 & 0.9 \end{bmatrix}$	$\begin{bmatrix} -0.12 & -0.011 \\ 0.01 & -0.11 \end{bmatrix}$	$\begin{bmatrix} -0.094 & -0.01 \\ 0.01 & -0.07 \end{bmatrix}$	$\begin{bmatrix} 0.1 & 0 \\ -0.1 & -0.1 \end{bmatrix}$	$\begin{bmatrix} 0 \\ 1 \end{bmatrix}$	$\begin{bmatrix} 0.1 & 0 \\ 0.09 & 0.1 \end{bmatrix}$	$\begin{bmatrix} 0.1 \\ 0.2 \end{bmatrix}$
2	$\begin{bmatrix} 0.89 & 0 \\ 0 & 0.92 \end{bmatrix}$	$\begin{bmatrix} -0.12 & -0.012 \\ 0.01 & -0.12 \end{bmatrix}$	$\begin{bmatrix} -0.092 & -0.013 \\ 0.01 & -0.07 \end{bmatrix}$	$\begin{bmatrix} 0.1 & 0 \\ -0.1 & -0.1 \end{bmatrix}$	$\begin{bmatrix} 0 \\ 1 \end{bmatrix}$	$\begin{bmatrix} 0 & 0.1 \\ 0 & 0.2 \end{bmatrix}$	$\begin{bmatrix} 0.1 \\ 0.2 \end{bmatrix}$

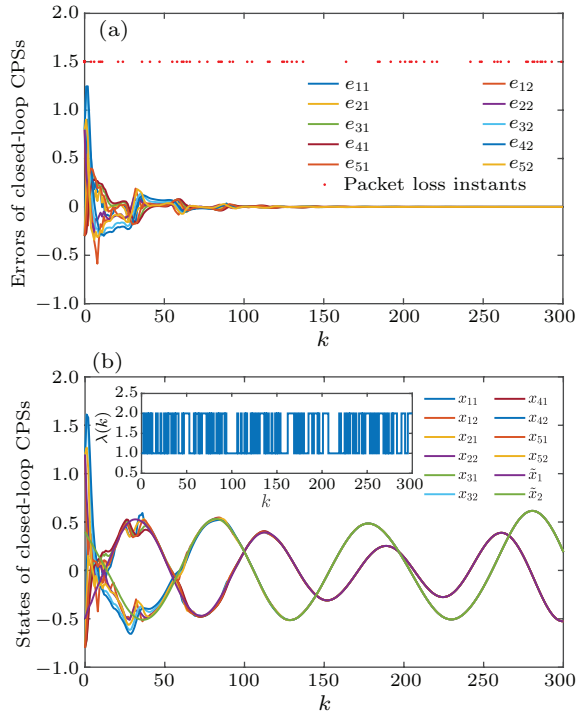


Fig. 8. (a) The curves of synchronization errors and packet loss instants. (b) The curves of node states and the evolution of system modes.

Assumed initial values of nodes in the interval $[-3,3]$, simulation results of closed-loop errors and states are exhibited in Fig. 8, where FTS can be realized for CPSs suffering from random packet losses. Controller signals are shown in Fig. 9 and the curves are step-like; this indicates that transmission only occurs at triggering sampling instants. Figure 10(a) gives the variation tendency of three dynamic variables $\Gamma_i(k)$ for $i = 1,2,5$, which vary together with the synchronization errors. The triggering performance of each node is displayed in Fig. 10(b).

In the following, the control performance for the situation of different parameter values will be discussed. As listed in Table 4, we compare the TR when the value of δ_i is set from 0 to 0.8. It is obvious that ATR decreases with the decline of δ_i monotonically, as described in Remark 1. Although a lower TR saves more computation resources, control ability may be affected because of receiving less available data.

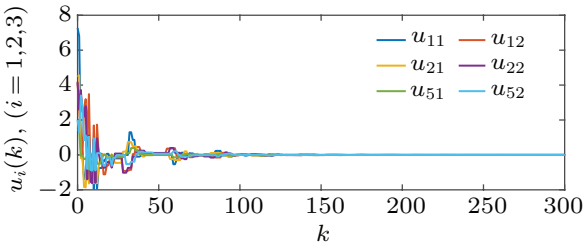


Fig. 9. The curves of controller signals.

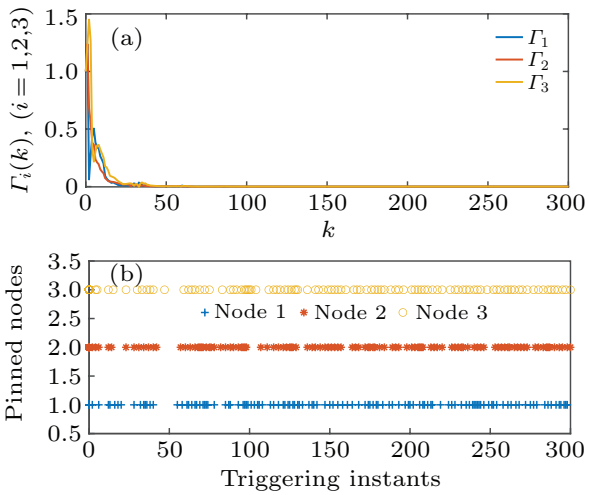


Fig. 10. (a) The evolutions of the dynamic variable $\Gamma_i(k)$ for $i = 1,2,5$. (b) The triggering instants of controllers 1, 2 and 5.

Table 4. A comparison of TRs under different values of δ_i.

	Node1	Node2	Node5	ATR
$\delta_i = 0$	100%	100%	100%	100%
$\delta_i = 0.3$	67.33%	67.67%	50.33%	61.78%
$\delta_i = 0.6$	43.67%	39%	35.33%	39.33%
$\delta_i = 0.8$	37%	33%	32.67%	34.22%

5. Conclusions

In this paper, the problem of finite-time dissipative synchronization control for TSFCPSs subject to semi-Markov switched parameters and packet losses has been addressed by applying the DDETM. Aiming to build the model of signals affected by random packet dropouts transmitting to the controller, combined with a compensation strategy, an equivalent prediction model is introduced to process the Bernoulli distributed time sequence. Based on an augmented mode-dependent LKF and ERCMI technique, the criterion of FTS with strictly dissipative performance has been deduced in terms of LMIs, which further solves the control gain matrices. The theoretical effectiveness and superiority are proved by two examples. In the future, the event-based control strategy will be extended to CPSs with more realistic problems, such as cyber-attack and sensor faults.

Acknowledgements

Project supported by the National Natural Science Foundation of China (Grant No. 62263005), Guangxi Natural Science Foundation (Grant No. 2020GXNSFDA238029), Laboratory of AI and Information Processing (Hechi University), Education Department of Guangxi Zhuang Autonomous Region (Grant No. 2022GXZDSY004), Innovation Project of Guangxi Graduate Education (Grant No. YCSW2023298), and Innovation Project of GUET Graduate Education (Grant Nos. 2022YCXS149 and 2022YCXS155).

References

[1] Qi W H, Hou Y K, Zong G D and Ahn C K 2021 *IEEE Trans. Circuits Syst. II, Express Briefs* **68** 2665
[2] Wang N and Li X J 2020 *IEEECAA Journal of Automatica Sinica* **7** 1215
[3] Xie X H, Hu S L and Liu Y G 2023 *IEEE Trans. Fuzzy Syst.* **31** 278
[4] Peng L H, Cao X H and Sun C Y 2021 *IEEE Trans. Cybern.* **51** 779
[5] Wang L, Cao X H, Zhang H, Sun C Y and Zheng W X 2022 *Automatica* **137** 110145
[6] Liu Z, Chen X and Yu J P 2023 *IEEE Trans. Industr. Inform.* **19** 3155
[7] Qi W H, Lv C Y, Zong G D, Cheng J and Shi K B 2022 *IEEE Trans. Circuits Syst. II, Express Briefs* **69** 159
[8] Sakthivel R, Kwon O M, Park M J, Choi S G and Sakthivel R 2022 *IEEE Trans. Fuzzy Syst.* **30** 3257
[9] Hu S L, Yue D, Peng C, Xie X P and Yin X X 2015 *Appl. Soft Comput.* **30** 400
[10] Qiu J B, Wang T, Sun K K, Rudas I and Gao H J 2022 *IEEE Trans. Fuzzy Syst.* **30** 1175
[11] Wu Y Q, Lu R Q, Shi P, Su H Y and Wu Z G 2018 *IEEE Trans. Fuzzy Syst.* **26** 782
[12] Tong S C, Li Y M, Feng G and Li T S 2011 *IEEE Trans. Syst. Man Cybern. Cybern.* **41** 1124
[13] Lian Z, Shi P and Lim C C 2023 *IEEE Trans. Industr. Inform.* **19** 6513
[14] Shen H, Xing M P, Huo S C, Wu Z G and Parl J H 2019 *Fuzzy Sets Syst.* **356** 113
[15] Tao J, Lu R Q, Shi P, Su H Y and Wu Z G 2017 *IEEE Trans. Cybern.* **47** 2377
[16] Lin W J, He Y, Zhang C K and Wu M 2020 *IEEE Trans. Neural Netw. Learn Syst.* **31** 5456
[17] Zhang L X, Yang T, Shi P and Liu M 2016 *IEEE Trans. Syst. Man Cybern. Syst.* **46** 1642
[18] Sakthivel R, Suveetha V T, Nithya V and Sakthivel R 2021 *Math. Comput. Simulat.* **185** 403
[19] Li Y M, Li K W and Tong S C 2020 *IEEE Trans. Neural Netw. Learn Syst.* **31** 2532
[20] Xu T L, Liu S and Wei G L 2022 *Int. J. Robust Nonlinear Control* **32** 3923
[21] Guan C X, Fei Z Y, Karimi H R and Shi P 2021 *IEEE Trans. Syst. Man Cybern. Syst.* **51** 2873
[22] Li Y, He Y, Zhang C K and Wu M 2023 *IEEE Trans. Cybern.* **53** 5459
[23] Song X N, Man J T, Ahn C K and Song S 2021 *IEEE Trans. Syst. Man Cybern. Syst.* **51** 3650
[24] Fei K F, Jiang M H and Zhang Y D 2021 *J. Intell. Fuzzy Syst.* **40** 1695
[25] Xue M, Yan H C, Zhang H, Li Z C, Chen S M and Chen C Y 2021 *IEEE Trans. Fuzzy Syst.* **29** 1052
[26] Chen X, Yin L Y, Liu Y T and Liu H 2019 *Chin. Phys. B* **28** 090701
[27] Ding S B and Wang Z S 2020 *Neural Netw.* **125** 31
[28] Rong N N, Wang Z S, Xie X P and Ding S B 2021 *IEEE Trans. Circuits Syst. II, Express Briefs* **68** 3296
[29] Zhu F Z, Park J H and Peng L 2022 *IEEE Trans. Signal Inf. Process. Netw.* **8** 258
[30] Xiao X Q, Park J H and Zhou L 2018 *Appl. Math. Comput.* **333** 344
[31] Ge X H, Han Q L and Wang Z D 2019 *IEEE Trans. Cybern.* **49** 171
[32] Deng Y H, Mo Z K and Lu H Q 2022 *Chin. Phys. B* **31** 020503
[33] Zheng X Y, Zhang H, Wang Z P, Zhang C Z and Yan H C 2022 *IEEE Trans. Fuzzy Syst.* **30** 2476
[34] Xiao M, Liu Z T and Su H Y 2022 *Chinese J. Aeronaut.* **34** 237
[35] Wang J, Xing M P, Cao J D, Park J H and Shen H 2023 *IEEE Trans. Neural Netw. Learn Syst.* **34** 278
[36] Jiang B P, Wu Z T and Karimi H R 2022 *Automatica* **142** 110357
[37] Kar A K, Dhar N K and Verma N K 2019 *IEEE Trans. Industr. Inform.* **15** 2101
[38] Xue M, Yan H C, Zhang H, Zhan X S and Shi K B 2022 *IEEE Trans. Cybern.* **52** 12759
[39] Chen H Y, Dong Q X, Li Z X and Wang Y F 2019 *Math. Probl. Eng.* **2019** 9624245
[40] Seuret A, Gouaisbaut F and Fridman E 2015 *IEEE Trans. Automat. Contr.* **60** 2740
[41] Jin L, He Y, Jiang L and Wu M 2018 *Inf. Sci.* **462** 357
[42] Sakthivel N, Pallavi S, Ma Y K and Vijayakumar V 2022 *Soft Comput.* **26** 8371
[43] Park P, Ko J W and Jeong C 2011 *Automatica* **47** 235